



저작자표시-비영리-변경금지 2.0 대한민국

이용자는 아래의 조건을 따르는 경우에 한하여 자유롭게

- 이 저작물을 복제, 배포, 전송, 전시, 공연 및 방송할 수 있습니다.

다음과 같은 조건을 따라야 합니다:



저작자표시. 귀하는 원저작자를 표시하여야 합니다.



비영리. 귀하는 이 저작물을 영리 목적으로 이용할 수 없습니다.



변경금지. 귀하는 이 저작물을 개작, 변형 또는 가공할 수 없습니다.

- 귀하는, 이 저작물의 재이용이나 배포의 경우, 이 저작물에 적용된 이용허락조건을 명확하게 나타내어야 합니다.
- 저작권자로부터 별도의 허가를 받으면 이러한 조건들은 적용되지 않습니다.

저작권법에 따른 이용자의 권리는 위의 내용에 의하여 영향을 받지 않습니다.

이것은 [이용허락규약\(Legal Code\)](#)을 이해하기 쉽게 요약한 것입니다.

[Disclaimer](#)

Doctoral Thesis

Multiantenna Downlink Interference Management for
Next Generation Mobile Networks

Youjin Kim

Department of Electrical Engineering

Ulsan National Institute of Science and Technology

2021

Multiantenna Downlink Interference Management for Next Generation Mobile Networks

Youjin Kim

Department of Electrical Engineering

Ulsan National Institute of Science and Technology


Multiantenna Downlink Interference Management for Next Generation Mobile Networks

A dissertation submitted to
Ulsan National Institute of Science and Technology
in partial fulfillment of the
requirements for the degree of
Doctor of Philosophy

Youjin Kim

12/09/2020

Approved by



Advisor

Sung Whan Yoon

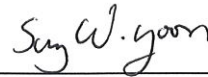
Multiantenna Downlink Interference Management for Next Generation Mobile Networks

Youjin Kim

This certifies that the dissertation of Youjin Kim is approved.

12/09/2020

Signature



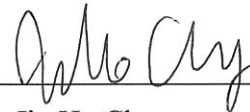
Advisor: Sung Whan Yoon

Signature



Hyun Jong Yang

Signature



Jin Ho Chung

Signature



Youngbin Im

Signature



Youngchol Choi

Abstract

In downlink multi-input single-output (MISO) networks, achieving optimal sum-rate with limited channel state information (CSI) is still a challenge even with a single user per cell. In this dissertation, three cooperative downlink multicell MISO beamforming schemes are proposed with highly limited information exchange among the base stations (BSs) to maximize the sum-rate. In the proposed schemes, each BS can design its beamforming vector with only local CSI based on limited information exchange on CSI. Unlike previous studies, the proposed beamforming designs are non-iterative and do not require any *vector* or *matrix* feedback but require only quantized scalar information.

In the first work, the beamforming vector at each BS is designed to minimize the sum of its *weighted* generating-interference (WGI) with local CSI and the aid of information exchange between the BSs. The generating-interference weight coefficients are designed in pursuit of increasing the sum-rate. Simulation results show that the proposed scheme outperforms the existing scheme in the mid to high signal-to-noise ratio (SNR) regime even with much reduced amount of information exchange via backhaul.

In the second work, the proposed beamforming design is based on the combination of the maximization of weighted signal-to-leakage-plus-noise ratio (WSLNR) and WGI. The weights in WSLNR and WGI are designed via choosing a proper set of users who shall be interference-free, which has never been endeavored in the literature. Though there have been extensive studies on downlink multicell beamforming, the proposed scheme closely achieves the optimal sum-rate bound in almost all SNR regime based on non-iterative optimization with lower amount of information exchange than existing schemes, which is justified by numerical simulations. In addition, the proposed scheme achieves a better trade-off between the amount of the information exchange and the sum-rate than existing schemes.

In the third work, a beamforming vector design based on a deep neural network (DNN) is proposed for multicell multi-input single-output channels with scalar information exchange and local CSI. The beamforming vectors are designed making zero generating-interference to the selected interference-free users (IFUs). The set of IFUs is chosen from the DNN based on supervised learning where the inputs can be obtained with only local CSI and limited scalar information exchange. Simulation results show that the DNN is well-trained in estimating the unknown CSI from the inputs with only local CSI in multicell networks.

©2018 IEEE. Reprinted, with permission, from [1]. ©2020 IEEE. Reprinted, with permission, from [2]. In reference to IEEE copyrighted material which is used with permission in this thesis, the IEEE does not endorse any of UNIST's products or services. Internal or personal use of this material is permitted. If interested in reprinting/republishing IEEE copyrighted material for advertising or promotional purposes or for creating new collective works for resale or redistribution, please go to http://www.ieee.org/publications_standards/publications/rights/rights_link.html to learn how to obtain a License from RightsLink. If applicable, University Microfilms and/or ProQuest Library, or the Archives of Canada may supply single copies of the dissertation.

Contents

I	Introduction	1
	1.1 Related Works	1
	1.2 Contribution	3
	1.2.1 First work	3
	1.2.2 Second work	3
	1.2.3 Third work	4
II	System model and Proposed Protocol	5
III	Proposed Beamforming Design 1 - Minimization of WGI	6
	3.1 Problem Formulation	6
	3.2 Step 1: Information Exchange Between BS's	7
	3.3 Step 2: Design of α_i Maximizing a Lower Bound of the Sum-Rate	7
	3.4 Scalar Value Quantization	10
	3.5 Bakchaul Signaling Comparison	12
	3.6 Spectral Efficiency Comparison	13
IV	Proposed Beamforming Design 2 - Selection of IFUs	19
	4.1 Beamforming vector design for $ \mathcal{F} = N_T$	20
	4.2 Beamforming vector design for $ \mathcal{F} = N_T - 1$	22
	4.2.1 BS n for $n \in \mathcal{N}_C \setminus \mathcal{F}$	23
	4.2.2 BS m for $m \in \mathcal{F}$	23
	4.3 Beamforming vector design for $ \mathcal{F} \leq N_T - 2$	25

4.4	Selection of \mathcal{F} : Design of β_{ij}	25
4.4.1	Tightness of the upper bound $\bar{R}_{\text{global}}^{[c]}$	28
4.4.2	Asymptotic performance of using $\bar{R}_{\text{global}}^{[c]}$	28
4.4.3	Performance of using $\bar{R}_{\text{global}}^{[c]}$ in finite SNR, N_T , and N_C	29
4.5	Information exchange	29
4.6	Quantization optimization	29
4.7	Information exchange protocol	31
4.8	Information exchange comparison	32
4.9	Extension to the Multiuser Case	32
4.9.1	Beamforming vector design for $ \mathcal{F}_M = N_T$	35
4.9.2	Beamforming vector design for $ \mathcal{F}_M = N_T - 1$	36
4.9.2.1	Design of \mathbf{w}_{n_r} for $n_r \in \mathcal{N}_W \setminus \mathcal{F}_M$:	36
4.9.2.2	Design of \mathbf{w}_{m_p} for $m_p \in \mathcal{F}$:	36
4.9.3	Beamforming vector design for $ \mathcal{F}_M \leq N_T - 2$	36
4.9.4	Selection of \mathcal{F}_M : Design of β_{i,k_l}	37
4.10	Numerical Simulations	37
V	Proposed Beamforming Design 3 - Selection of IFUs with DNN	48
5.1	Input data	48
5.2	Offline training data	48
5.3	Selection of \mathcal{F} using DNN	48
5.4	Numerical Simulations	49
VI	Conclusion	52
6.1	First work	52
6.2	Second work	52
6.3	Third work	53

References 54

List of Figures

1	Channel model of BS i in the MISO downlink network	5
2	Per-cell average rate versus SNR for $N_T = 2$ and $N_C = 3$	16
3	Per-cell average rate versus SNR for $N_T = 4$ and $N_C = 7$	17
4	Per-cell average rate versus SNR for $N_T = 2$, $N_C = 3$, and the antenna correlation matrix \mathbf{R}_2	18
5	Per-cell average rate versus SNR for $N_T = 4$, $N_C = 7$, and the antenna correlation matrix \mathbf{R}_4	18
6	Average per-cell sum-rate and the average number of IFUs versus SNR for $N_T = 4$ and $N_C = 5$	20
7	Illustration of the proposed multicell beamforming vector design	26
8	PDFs of $r_m^{[c]}$ for $N_T = 4$, and $N_C = 7$	31
9	Example of the overall beamforming vectors design and information exchange protocol for $N_T = 3$, $N_C = 4$, and $\mathcal{A} = \{1, 2, 3\}$	33
10	Per-cell average $R_{\text{global}}^{[c]}$ and $\bar{R}_{\text{global}}^{[c]}$ versus SNR for $N_T = 4$ and $N_C = 7$	34
11	Per-cell average rate versus SNR for $N_T = 4$ and $N_C = 7$	41
12	Per-cell average rate versus SNR for $N_T = 8$ and $N_C = 9$	42
13	Per-cell average rate versus SNR of the proposed scheme for $N_T = 4$, $N_C = 7$, and $N_f = 42$	43
14	Per-cell average rate versus SNR of the proposed scheme for $N_T = 8$, $N_C = 9$, and $N_f = 250$	43

15	Probability that each α value is chosen in the proposed scheme for SNR of -5~25dB, $N_T = 8$, and $N_C = 9, 10, 11, 12$	44
16	Relative per-cell average rate normalized to that of 'Global-unquantized' versus the amount of required information exchange for SNR of -5~25dB	45
17	(a) The per-cell average rate versus transmission power and (b) the cell configuration with a single user per cell for $N_T = 4$ and $N_C = 7$	46
18	(a) The per-cell average rate versus transmission power and (b) the cell configuration for $N_T = 4$, $N_C = 7$, and $N_U = 2$	47
19	Proposed DNN architecture	49
20	Accuracy of the proposed scheme for the test set versus epoch	50
21	Per-cell average rate versus transmit power of BSs	51

List of Tables

1	Codebooks designed by Algorithm 1	12
2	Amount of required backhaul signaling	13
3	Achievable rates table for all the IFU selection cases for $N_T = 3$ and $N_C = 4$. . .	30
4	Amount of required information exchange	34
5	Amount of required computational complexity in order of flops	39

I Introduction

In multicell networks, intercell interference management is of great importance to increase the total sum-rate. One of the key enablers of the next generation mobile communications is cell densification, through which improved channel gain is expected due to reduced distance between the transmitter and receiver. In dense multicell networks, the signal-to-interference-plus-noise ratio (SINR) cannot grow unless the interference signals are kept weak enough compared to the desired channel gain [3]. If the transmitter is equipped with multiple antennas, intercell interference can be significantly mitigated or even cancelled via spatial transmit beamforming [1, 4–12]. The interference alignment framework [13,14] achieves asymptotically optimal multiplexing gain based on global channel state information (CSI) at the cost of excessive use of frequency- or time-domain signal extension, but with no guarantee of optimal sum-rate achievability. Though massive multi-input multi-output (MIMO) employed at the transmitter provide significant spectral efficiency gain [15,16], the number of transmit antennas even at base stations (BSs) is often limited by up to 8 in the pervasive conventional mobile networks [17].

In the downlink scenario, if information exchange for global CSI is allowed among the BSs via direct link, coordinated multi-point (CoMP) can be employed [12]. CoMP techniques can be classified into two categories: i) joint transmission and ii) coordinated beamforming. In the joint transmission, the data streams designated to a single user are jointly transmitted from multiple BSs simultaneously, which requires continuous and excessive use of backhaul or information exchange among the BSs. In coordinated beamforming, only the beamforming vectors are jointly optimized, and each user's data streams are transmitted by a single serving BS. In practical environment with limited direct link capacity [18], coordinated beamforming is more preferable than joint transmission, since the former requires information exchange among the BSs only if the channel state significantly changes. In this paper, the focus is on the coordinated downlink multi-input single-output (MISO) beamforming design with limited direct link capacity. With a wireless direct link, which is put on the highest priority by 3GPP, the capacity is limited by 10-100Mbps typically. In such a case, highly limited information exchange is required, particularly in dense networks. Although the MISO multicell network is a well-studied area, achieving the optimal sum-rate with limited information exchange on CSI is still a major challenge.

1.1 Related Works

With global CSI, coordinated beamforming offers optimal multiplexing gain [6,10,19], an optimal Pareto rate boundary [9], or a significant sum-rate gain over the conventional distributed beamforming [20, 21]. However, in MISO networks, the amount of CSI information exchange in general increases as the number of transmit antennas grows, which make them difficult to be implemented in systems with limited direct link or backhaul capacity.

Several studies have proposed cooperative beamforming methods with vector quantization to reduce the amount of information exchange [1, 5, 22–32]. In [5,26], separate and joint vector

quantization methods for desired and interference channels are proposed to maximize the sum-rate. In [24], coordinated regularized multiuser MISO precoding is proposed based on vector-quantized global CSI assuming massive antennas at the BSs. In [32], joint processing coordinated multi-point transmission for downlink beamforming is proposed based on vector quantization in pursuit of maximizing the weighted sum-rate. Interference alignment with vector quantization of CSI is proposed in [28], and the impact of imperfect CSI in interference alignment is derived in [33]. Rate loss of the coordinated zero-forcing precoding due to the vector quantization of CSI in time-varying channels is derived in [29]. Adaptive feedback bits allocation methods across cells [22, 30] and across users [31] are proposed to minimize the rate loss due to vector quantization error. However, with the vector quantization, the number of quantization bits increases linearly with respect to the number of antennas to achieve the same rate.

Distributed beamforming also has been proposed based only on local CSI requiring no information exchange [4, 9, 34–39]. In [9], the condition of beamforming vector which corresponds to Pareto’s optimal rate boundary is derived for a multicell MISO channel with local CSI. However, no closed-form solution of beamforming vector is derived. In [37], a simple MIMO downlink precoding is proposed in a single cell maximizing each user’s signal-to-leakage-plus-noise ratio (SLNR)¹ while decoupling each user’s beamforming vector design. In [34, 36, 38, 39], the SLNR-maximizing beamforming scheme is applied to the multicell MISO channel, and the achievability of Pareto’s optimal rate bound is discussed. The same idea was extended in [4, 35] to the multicell MISO network where each user is served by all the BSs assuming each user’s data being shared by all the BSs, i.e., coordinated multi-point joint transmission. Statistical beamforming design schemes robust to instantaneous CSI have also been proposed based only on the second order statistics of local CSI [4, 23]. However, the sum-rate of these SLNR-maximizing schemes with only local CSI is far below the channel capacity of the multicell MISO channel, especially in high-SNR regime.

Iterative beamforming design approaches, in which the BSs update their beamforming vectors iteratively exchanging interference pricing measures with other BSs or users, have been proposed in pursuit of maximizing the sum-rate of the two-user MIMO interference channel [40] and minimizing transmission power of the multicell MISO channel [41–43] with the use of limited information exchange. In the scheme proposed in [44], beamforming vectors, receive equalizers, and weight coefficients are designed iteratively between the transmitters and receivers. However, it requires excessive amount of information exchange due to the vector information exchange about the beamforming vectors. Furthermore, iterative optimization can significantly increase the overhead of information exchange for convergence of the solutions.

In [45], the beamforming vectors design based on neural network is proposed. However, the optimal beamforming solution to the sum-rate maximization problem is still unknown.

¹The terminology is also known as signal-to-generating-interference-and-noise ratio (SGINR) [36] or distributed virtual SINR [4].

1.2 Contribution

In this dissertation, we propose non-iterative cooperative downlink beamforming schemes in multicell MISO networks, each cell of which consists of a BS with multiple antennas and a user with a single antenna, based on local CSI with limited information exchange of scalar values. The contribution in summary is as follows:

1.2.1 First work

- In the proposed scheme, the beamforming vector at each BS is designed to minimize the sum of weighted generating-interference (WGI) based on local CSI with a few bits of *quantized scalar* information exchange among the BSs. Note that the amount of scalar information to be exchanged via backhaul does not increase with respect to the number of antennas, thus making it easier to be implemented.
- The generating-interference (GI) weight coefficients are determined in pursuit of increasing the sum-rate. Simulation results show that the proposed scheme outperforms the distributed iterative beamforming design [44] even with much reduced backhaul signaling in the mid to high signal-to-noise ratio (SNR).

1.2.2 Second work

- We first give inspiration that the sum-rate maximization may be achieved by choosing a proper set of users and making them interference-free. From this inspiration, we propose a novel multicell beamforming design based on the mixture of the maximization of weighted signal-to-leakage-plus-noise ratio (WSLNR) and the minimization of weighted generating-interference (WGI). Unlike previous related studies, where the SLNR or generating-interference (GI) formulation with identical weights was used, we focus on the design of the weights in WSLNR and WGI via choosing a proper set of interference-free users (IFUs).
- For each selection on the number of IFUs, we provide an information exchange protocol with limited direct link capacity, and present an adaptive beamforming design scheme. In the proposed protocol, only scalar information, not vector CSI, is exchanged, and hence the amount of information exchange does not grow for increasing number of antennas.
- Then, a scalar quantization method for the information to be exchanged is derived, based on which quantitative evaluation of the amount of information exchange is provided compared with existing schemes.
- We derive conditions of system parameters for which the optimal sum-rate is asymptotically achievable with the proposed scheme. We also confirm by extensive simulations that the proposed scheme closely achieves the optimal sum-rate bound for almost all the SNR regime requiring less information exchange compared to the existing schemes. Although

there have been extensive studies on multicell MISO beamforming, to the best of authors' knowledge, this is the first non-iterative beamforming design that achieves the optimal sum-rate bound even with the lowest information exchange overhead.

1.2.3 Third work

- We propose a DNN-based beamforming design scheme to maximize the sum-rate. The DNN is used to capture the partial channel information from the shared scalar information with local CSI and choose the proper set of IFUs. With the selected set of IFUs from the DNN, all BSs design beamforming vectors based on the mixture of maximization WSLNR and minimization WGI according to the inspiration of [2].
- Simulation results show that the proposed scheme closely achieves the optimal sum-rate bound and higher sum-rate than the existing schemes with local CSI regardless for all considered the transmit power in the small cell network showing that the DNN is well-trained.

II System model and Proposed Protocol

It is assumed that each cell is composed of a single BS and user assuming frequency-, code-, or time-division multi-user orthogonal multiplexing. Each small cell BS is assumed to have N_T antennas, whereas each user has a single antenna. The number of cells considered is denoted by N_C , and it is assumed that $N_T < N_C$ and $N_T \geq 2$. The channel vector from the i -th BS (referred to as BS i henceforth) to the user in the j -th cell (referred to as user j henceforth) is denoted by $\mathbf{h}_{ij} \in \mathbb{C}^{N_T \times 1}$. Block fading and time-division duplexing with channel reciprocity are assumed. Resorting to channel reciprocity, each BS is assumed to have local CSI at the transmitter [4], i.e., BS i has the information of \mathbf{h}_{ij} , $j \in \{1, \dots, N_C\} \triangleq \mathcal{N}_C$, as shown in Fig. 1.

The beamforming vector at BS i is denoted by $\mathbf{w}_i \in \mathbb{C}^{N_T \times 1}$, where $\|\mathbf{w}_i\|^2 \leq 1$. The received signal at user i is written by

$$y_i = \underbrace{\mathbf{h}_{ii}^H \mathbf{w}_i x_i}_{\text{desired signal}} + \underbrace{\sum_{k \in \mathcal{N}_C \setminus \{i\}} \mathbf{h}_{ki}^H \mathbf{w}_k x_k}_{\text{intercell interference}} + z_i, \quad (1)$$

where x_l is the unit-variance transmit symbol at BS l , $l \in \mathcal{N}_C$, and z_i is the additive white Gaussian noise (AWGN) at user i with zero-mean and variance of N_0 . Thus, the corresponding SINR is expressed by

$$\gamma_i = \frac{|\mathbf{h}_{ii}^H \mathbf{w}_i|^2}{\sum_{k \in \mathcal{N}_C \setminus \{i\}} |\mathbf{h}_{ki}^H \mathbf{w}_k|^2 + N_0}, \quad (2)$$

and the achievable sum-rate is given by

$$R = \sum_{i=1}^{N_C} \log(1 + \gamma_i). \quad (3)$$

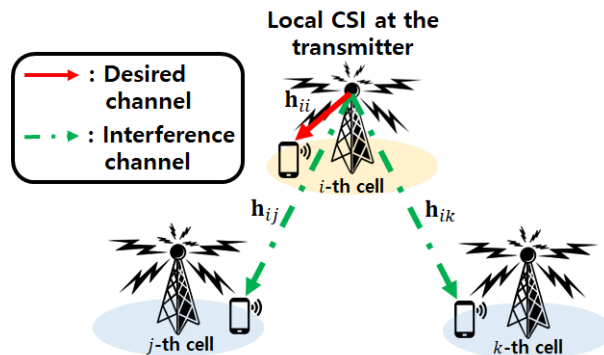


Figure 1: Channel model of BS i in the MISO downlink network

III Proposed Beamforming Design 1 - Minimization of WGI

3.1 Problem Formulation

Let us consider the beamforming design of BS i . The WGI at the BS i is defined as

$$\Omega_i(\mathbf{w}_i, \boldsymbol{\alpha}_i) = \sum_{j=1, j \neq i}^{N_C} \alpha_{ij} |\mathbf{h}_{ij}^H \mathbf{w}_i|^2, \quad (4)$$

where $\alpha_{ij} \geq 0$, $\sum_{j=1, j \neq i}^{N_C} \alpha_{ij} = 1$, and $\boldsymbol{\alpha}_i \triangleq [\alpha_{i1}, \dots, \alpha_{i(i-1)}, \alpha_{i(i+1)}, \dots, \alpha_{iN_C}]$. Here, the interference weight α_{ij} accounts for the relative emphasis on each interference channel. When minimizing (4), large α_{ij} leads to generating-interference (GI) from BS i to user j being more reduced compared to the other GI from BS i . To minimize the WGI, the beamforming vector at BS i is designed such that

$$\mathbf{w}_i = \arg_{\mathbf{w}} \min \Omega_i(\mathbf{w}, \boldsymbol{\alpha}_i), \text{ s.t. } \|\mathbf{w}\|^2 = 1. \quad (5)$$

Note that Ω_i can be expressed as

$$\Omega_i = \|\mathbf{G}_i \mathbf{w}_i\|^2, \quad (6)$$

where

$$\mathbf{G}_i(\boldsymbol{\alpha}_i) \triangleq [\sqrt{\alpha_{i1}} \mathbf{h}_{i1}, \dots, \sqrt{\alpha_{i(i-1)}} \mathbf{h}_{i(i-1)}, \sqrt{\alpha_{i(i+1)}} \mathbf{h}_{i(i+1)}, \dots, \sqrt{\alpha_{iN_C}} \mathbf{h}_{iN_C}]^H. \quad (7)$$

Let us denote the singular value decomposition of the matrix $\mathbf{G}_i \in \mathbb{C}^{(N_C-1) \times N_T}$ as $\mathbf{G}_i = \mathbf{U}_i \boldsymbol{\Sigma}_i \mathbf{V}_i^H$, where $\mathbf{U}_i \in \mathbb{C}^{(N_C-1) \times (N_C-1)}$ and $\mathbf{V}_i \in \mathbb{C}^{N_T \times N_T}$ consist of orthogonal columns, and $\boldsymbol{\Sigma}_i \in \mathbb{C}^{(N_C-1) \times N_T}$ is a diagonal matrix composed of the singular values of \mathbf{G}_i . The solution for the problem (5) is given by $\mathbf{w}_i = \mathbf{v}_i^{[N_T]}$, where $\mathbf{v}_i^{[N_T]}$ is the N_T -th column of \mathbf{V}_i , associated with the minimum singular value of \mathbf{G}_i . The solution of (5), however, is not unique, since $c \mathbf{v}_i^{[N_T]}$ also could be the solution for the problem (5), where c is an arbitrary complex number and $|c|^2 = 1$. However, all the solutions $c \mathbf{v}_i^{[N_T]}$ have the same WGI since $|c|^2 = 1$, and hence, the unique solution can be obtained without loss of generality as follows:

$$\mathbf{w}_i^* = \frac{\bar{v}_{i,1}^{[N_T]}}{|v_{i,1}^{[N_T]}|} \mathbf{v}_i^{[N_T]}, \quad (8)$$

where $v_{i,k}^{[N_T]}$ is the k -th element of $\mathbf{v}_i^{[N_T]}$, and $\bar{v}_{i,k}^{[N_T]}$ is the complex conjugate of $v_{i,k}^{[N_T]}$. Let us denote the set \mathcal{A} by $\mathcal{A} \triangleq \left\{ \mathbf{a} : \sum_{m=1}^{N_C-1} a_m = 1, \mathbf{a} = [a_1, \dots, a_{N_C-1}] \in \mathbb{R}_{\geq 0}^{N_C-1} \right\}$. Then, since for any given $\boldsymbol{\alpha}_i \in \mathcal{A}$, a unique \mathbf{G}_i is defined from (7), and thus a unique \mathbf{w}_i^* is obtained from (8). Therefore, the function $\boldsymbol{\omega}_i : \mathcal{A} \rightarrow \mathbb{C}^{N_T}$ can be defined by

$$\boldsymbol{\omega}_i(\boldsymbol{\alpha}_i) = \mathbf{w}_i^*. \quad (9)$$

Remark 1. In fact, for any given α_{ij} , $j = 1, \dots, i-1, i+1, \dots, N_C$, inserting $r \cdot \alpha_{ij}$ with any positive real value r into (7) leads to the same right singular matrix \mathbf{V}_i and the same beamforming

vector \mathbf{w}_i^* . Thus, the constraint $\sum_{j=1, j \neq i}^{N_C} \alpha_{ij} = 1$ is not necessarily needed. Nevertheless, posing this constraint does not lose any generality of the problem, while providing us with mathematical convenience in deriving the lower-bound of the sum-rate as shown later in Lemma 1.

In what follows, a protocol to design α_i with local CSI and limited backhaul signaling in pursuit of maximizing the sum-rate is proposed.

3.2 Step 1: Information Exchange Between BS's

As an initialization step, with only local CSI, BS j calculates its preparatory beamforming vector $\hat{\mathbf{w}}_i$ from

$$\hat{\mathbf{w}}_i = \arg_{\mathbf{w}} \min \sum_{j=1, j \neq i}^{N_C} |\mathbf{h}_{ij}^H \mathbf{w}|^2. \quad (10)$$

That is, $\hat{\mathbf{w}}_i$ is the beamforming vector merely minimizing the sum of GI [46]. Note that (10) includes only the outgoing channels from BS i , and thus can be solved at BS i only with local CSI. Then, BS i shares the scalars $|\mathbf{h}_{il}^H \hat{\mathbf{w}}_i|^2$, $l \in \mathcal{N}_C$, with all other BSs via backhaul. Therefore, the amount of the information to be exchanged via backhaul does not increase with respect to the number of antennas. To consider limited backhaul capacity, scalar quantization shall be considered in Section 3.4.

3.3 Step 2: Design of α_i Maximizing a Lower Bound of the Sum-Rate

Now, let us rewrite the sum-rate maximization problem as

$$\max_{\mathbf{w}_1, \dots, \mathbf{w}_{N_C}} \sum_{l=1}^{N_C} \log(1 + \rho_l) = \max_{\mathbf{w}_i} R_i(\mathbf{w}_i), \quad (11)$$

where

$$R_i(\mathbf{w}_i) = \max_{\mathbf{w}_1, \dots, \mathbf{w}_{i-1}, \mathbf{w}_{i+1}, \dots, \mathbf{w}_{N_C}} \sum_{l=1}^{N_C} \log(1 + \rho_l). \quad (12)$$

Since \mathbf{w}_i is a function of α_i as in (9), the following modified formulation is posed:

$$\max_{\alpha_i} R_i(\omega_i(\alpha_i)). \quad (13)$$

Since ρ_i in (2) is a function of all the beamforming vectors, i.e., function of $\alpha_1, \dots, \alpha_{N_C}$, global CSI is required to compute $R_i(\mathbf{w}_i)$ in (12) and solve (13).

To circumvent the requirement of the global CSI acquisition, we propose to maximize a lower-bound on the sum-rate, which obviously results in an improved sum-rate. Specifically, we convert the sum-rate-maximizing problem into the maximization of a lower-bound on the sum-rate to separate the design of α_i from the design of α_j , $j \neq i$. To design α_i , let us denote the modified SINRs of user i and user j , $j \neq i$, where $|\mathbf{h}_{ki}^H \mathbf{w}_k|^2$ and $|\mathbf{h}_{kj}^H \mathbf{w}_k|^2$, $k \neq i$, are substituted by $|\mathbf{h}_{ki}^H \hat{\mathbf{w}}_k|^2$ and $|\mathbf{h}_{kj}^H \hat{\mathbf{w}}_k|^2$, by $\rho_i^{[i]}$ and $\rho_j^{[j]}$, respectively. Note that $|\mathbf{h}_{ki}^H \hat{\mathbf{w}}_k|^2$ and $|\mathbf{h}_{kj}^H \hat{\mathbf{w}}_k|^2$ are calculated and shared in step 1.

Then, $\rho_i^{[i]}$ and $\rho_j^{[i]}$ for $j \neq i$ is given by

$$\rho_i^{[i]}(\boldsymbol{\omega}_i(\boldsymbol{\alpha}_i)) = \frac{|\mathbf{h}_{ii}^H \boldsymbol{\omega}_i(\boldsymbol{\alpha}_i)|^2}{\sum_{j=1, j \neq i}^{N_C} |\mathbf{h}_{ji}^H \hat{\mathbf{w}}_j|^2 + N_0}, \quad (14)$$

$$\rho_j^{[i]}(\boldsymbol{\omega}_i(\boldsymbol{\alpha}_i)) = \frac{|\mathbf{h}_{jj}^H \hat{\mathbf{w}}_j|^2}{|\mathbf{h}_{ij}^H \boldsymbol{\omega}_i(\boldsymbol{\alpha}_i)|^2 + \sum_{k=1, k \neq i, j}^{N_C} |\mathbf{h}_{kj}^H \hat{\mathbf{w}}_k|^2 + N_0}. \quad (15)$$

In other words, $\rho_i^{[i]}$ and $\rho_j^{[i]}$ can be viewed as the estimates of the SINRs for user i and user j , respectively, in BS i 's perspective. We have for all $\boldsymbol{\omega}_i(\boldsymbol{\alpha}_i)$

$$R_i(\boldsymbol{\omega}_i(\boldsymbol{\alpha}_i)) \geq \sum_{l=1}^{N_C} \log \left(1 + \rho_l^{[i]}(\boldsymbol{\omega}_i(\boldsymbol{\alpha}_i)) \right), \quad (16)$$

because for given $\boldsymbol{\omega}_i(\boldsymbol{\alpha}_i)$, $R_i(\boldsymbol{\omega}_i(\boldsymbol{\alpha}_i))$ is maximized with respect to $\mathbf{w}_1, \dots, \mathbf{w}_{i-1}, \mathbf{w}_{i+1}, \dots, \mathbf{w}_{N_C}$ as in (12), whereas fixed $\mathbf{w}_k = \hat{\mathbf{w}}_k$, $k \neq i$, is applied to calculate $\sum_{l=1}^{N_C} \log \left(1 + \rho_l^{[i]}(\boldsymbol{\omega}_i(\boldsymbol{\alpha}_i)) \right)$.

Now, to bound $R_i(\boldsymbol{\omega}_i(\boldsymbol{\alpha}_i))$ further, the following lemma is established.

Lemma 1. *Let us denote*

$$\hat{\mathbf{G}}_i \triangleq [\mathbf{h}_{i1}, \dots, \mathbf{h}_{i(i-1)}, \mathbf{h}_{i(i+1)}, \dots, \mathbf{h}_{iN_C}]^H. \quad (17)$$

Then, the WGI in the proposed scheme at BS i , $\|\mathbf{G}_i \boldsymbol{\omega}_i(\boldsymbol{\alpha}_i)\|^2$, is bounded by the GI in the min-GI scheme as

$$\|\mathbf{G}_i \boldsymbol{\omega}_i(\boldsymbol{\alpha}_i)\|^2 \leq \|\hat{\mathbf{G}}_i \hat{\mathbf{w}}_i\|^2. \quad (18)$$

Proof. Let \mathbf{A} and \mathbf{B} be complex $m \times n$ matrices and let $q = \min\{m, n\}$. Then, the multiplicative Schur-Horn inequality (also known as Weyl inequality) [47] gives us

$$\lambda_{j+k-1}(\mathbf{A}\mathbf{B}^H) \leq \lambda_j(\mathbf{A})\lambda_k(\mathbf{B}), \quad (19)$$

where $\lambda_i(\cdot)$ denotes the i -th singular value of a matrix, $1 \leq j, k \leq q$, and $j+k-1 \leq q$. Since $\hat{\mathbf{G}}_i$ is a tall or square matrix when $N_C > N_T$, let us define $\mathbf{\Pi}_i$ by

$$\mathbf{\Pi}_i \triangleq [\mathbf{G}_i, \mathbf{0}_{(N_C-1) \times (N_C-1-N_T)}] \in \mathbb{C}^{(N_C-1) \times (N_C-1)}. \quad (20)$$

Then, $\hat{\mathbf{\Pi}}_i$ can be obtained by substituting \mathbf{G}_i in (20) as $\hat{\mathbf{G}}_i$. Defining

$$\mathbf{\Xi}_i = \text{diag} \left(\sqrt{\alpha_{i1}}, \dots, \sqrt{\alpha_{i(i-1)}}, \sqrt{\alpha_{i(i+1)}}, \dots, \sqrt{\alpha_{iN_C}} \right), \quad (21)$$

we have $\mathbf{\Pi}_i = \mathbf{\Xi}_i \hat{\mathbf{\Pi}}_i$. Inserting $\mathbf{A} = \mathbf{\Xi}_i$ and $\mathbf{B} = \hat{\mathbf{\Pi}}_i^H$ into (19) gives us

$$\lambda_{j+k-1} \left(\mathbf{\Xi}_i \hat{\mathbf{\Pi}}_i \right) \leq \lambda_j(\mathbf{\Xi}_i) \lambda_k \left(\hat{\mathbf{\Pi}}_i^H \right), \quad (22)$$

for $1 \leq j, k \leq N_T, j+k-1 \leq N_T$. Thus, for $j=1$, we have

$$\lambda_k(\mathbf{\Pi}_i) \leq \lambda_1(\mathbf{\Xi}_i) \lambda_k(\hat{\mathbf{\Pi}}_i^H) \leftrightarrow \lambda_k(\mathbf{G}_i) \leq \lambda_1(\mathbf{\Xi}_i) \lambda_k(\hat{\mathbf{G}}_i^H), \text{ for } 1 \leq k \leq N_T, \quad (23)$$

where (23) follows from the fact that $\lambda_{N_T}(\hat{\mathbf{G}}_i^H) = \lambda_{N_T}(\hat{\mathbf{G}}_i)$ and that the largest singular value of $\mathbf{\Xi}_i$ is bounded by $\lambda_1(\mathbf{\Xi}_i) \leq 1$, since $\sqrt{\alpha_{ij}} \leq 1$. Therefore, we can get $\lambda_k(\mathbf{G}_i) \leq \lambda_k(\hat{\mathbf{G}}_i)$, and inserting $k = N_T$ yields

$$\lambda_{N_T}(\mathbf{G}_i) = \|\mathbf{G}_i \boldsymbol{\omega}_i(\boldsymbol{\alpha}_i)\| \leq \lambda_{N_T}(\hat{\mathbf{G}}_i) = \|\hat{\mathbf{G}}_i \hat{\mathbf{w}}_i\|, \quad (24)$$

which proves the lemma. \square

In addition, using Lemma 1, the following theorem is established to derive a lower-bound of the sum-rate.

Theorem 1. For given $\boldsymbol{\alpha}_i$, we have

$$R_i(\boldsymbol{\omega}_i(\boldsymbol{\alpha}_i)) \geq \sum_{j=1, j \neq i}^{N_C} \log(1 + \alpha_{ij} C_{ij}), \quad (25)$$

where

$$C_{ij} = \frac{|\mathbf{h}_{jj}^H \hat{\mathbf{w}}_j|^2}{\|\hat{\mathbf{G}}_i \hat{\mathbf{w}}_i\|^2 + \sum_{k=1, k \neq i, j}^{N_C} |\mathbf{h}_{kj}^H \hat{\mathbf{w}}_k|^2 + N_0}. \quad (26)$$

Proof. Since $\sum_{j=1, j \neq i}^{N_C} \alpha_{ij} |\mathbf{h}_{ij}^H \mathbf{w}_i|^2 = \|\mathbf{G}_i \boldsymbol{\omega}_i\|^2$ by (4) and (6), from Lemma 1, we have

$$\|\hat{\mathbf{G}}_i \hat{\mathbf{w}}_i\|^2 \geq \|\mathbf{G}_i \boldsymbol{\omega}_i(\boldsymbol{\alpha}_i)\|^2 \geq \alpha_{ij} |\mathbf{h}_{ij}^H \boldsymbol{\omega}_i(\boldsymbol{\alpha}_i)|^2. \quad (27)$$

Then, for given $\boldsymbol{\alpha}_i$, we can obtain a lower bound on $\rho_j^{[i]}$ as followings:

$$\rho_j^{[i]}(\boldsymbol{\omega}_i(\boldsymbol{\alpha}_i)) = \frac{|\mathbf{h}_{jj}^H \hat{\mathbf{w}}_j|^2}{|\mathbf{h}_{ij}^H \boldsymbol{\omega}_i(\boldsymbol{\alpha}_i)|^2 + \sum_{k=1, k \neq i, j}^{N_C} |\mathbf{h}_{kj}^H \hat{\mathbf{w}}_k|^2 + N_0} \quad (28)$$

$$\geq \frac{|\mathbf{h}_{jj}^H \hat{\mathbf{w}}_j|^2}{\frac{\|\hat{\mathbf{G}}_i \hat{\mathbf{w}}_i\|^2}{\alpha_{ij}} + \sum_{k=1, k \neq i, j}^{N_C} |\mathbf{h}_{kj}^H \hat{\mathbf{w}}_k|^2 + N_0} \quad (29)$$

$$\geq \alpha_{ij} C_{ij}, \quad (30)$$

where (29) follows from (27), and (30) follows from $0 \leq \alpha_{ij} \leq 1$. Here, C_{ij} is defined in (26). Therefore, we further have

$$R(\boldsymbol{\omega}_i(\boldsymbol{\alpha}_i)) \geq \sum_{j=1, j \neq i}^{N_C} \log\left(1 + \rho_j^{[i]}(\boldsymbol{\omega}_i(\boldsymbol{\alpha}_i))\right) \quad (31)$$

$$\geq \sum_{j=1, j \neq i}^{N_C} \log(1 + \alpha_{ij} C_{ij}), \quad (32)$$

where (31) follows from (16), and (32) follows from (30). \square

Note that BS i can compute C_{ij} in (26) using the exchanged information. From (25), α_{ij} which maximizes the lower bound of the sum-rate can be obtained as

$$\boldsymbol{\alpha}_i^* = \arg \max_{\boldsymbol{\alpha}_i} \sum_{j=1, j \neq i}^{N_C} \log(1 + \alpha_{ij} C_{ij}) \longrightarrow \alpha_{ij}^* = \left[\gamma - \frac{1}{C_{ij}} \right]^+, \quad (33)$$

where $[\chi]^+ = \max(\chi, 0)$ and γ can be calculated from $\sum_{j=1, j \neq i}^{N_C} \alpha_{ij}^* = 1$. Note that the numerator of C_{ij} defined in (26) is the desired signal of the j -th cell with the min-GI beamforming design, and the denominator includes the interference signal to the j -th cell with the min-GI beamforming design. Thus, α_{ij} is designed by (33) considering both of the desired signal and the intercell interference signal which are related to the SINR, thus improving the lower-bound of the sum-rate.

Finally, inserting $\boldsymbol{\alpha}_i^*$ obtained from (33) into (4), the beamforming vector at BS i can be obtained from

$$\mathbf{w}_i = \boldsymbol{\omega}_i(\boldsymbol{\alpha}_i^*). \quad (34)$$

Note that $\hat{\mathbf{w}}_i$ in (10) can be obtained by BS i with only local CSI. In addition, C_{ij} in (33) can also be calculated with exchanged information and only local CSI by definition of (26). For given $\boldsymbol{\alpha}_i^*$ obtained from solving (33), the solution of \mathbf{w}_i in (34) can be immediately computed by establishing \mathbf{G}_i for given $\boldsymbol{\alpha}_i^*$ as in (7) and computing \mathbf{w}_i^* from (8), which requires only local CSI. Therefore, though the proposed scheme obtains a sub-optimal solution that improves the lower bound of the sum-rate, it provides a nice compromise between the amount of backhaul signaling and the sum-rate performance, which shall be shown by numerical results in Section 3.6.

3.4 Scalar Value Quantization

To minimize the amount of the use of backhaul for exchanging $\left| \mathbf{h}_{ij}^H \hat{\mathbf{w}}_i \right|^2$, $i, j \in \mathcal{N}_C$, an M -level non-uniform quantization is considered. Let us denote the quantization points by y_j , $j = 1, \dots, M$, and the boundaries by b_k , $k = 1, \dots, M - 1$. The following theorem establishes the necessary condition for a non-uniform quantization minimizing the mean-square quantization error (MSQE).

Theorem 2. *A necessary condition of minimizing the MSQE is given by*

$$y_j = \frac{[tF(t)]_{b_{j-1}}^{b_j} - \int_{b_{j-1}}^{b_j} F(t) dt}{[F(t)]_{b_{j-1}}^{b_j}}, \quad (35)$$

where $[g(x)]_{\delta_2}^{\delta_1} \triangleq g(\delta_1) - g(\delta_2)$ and $F(t)$ is the cumulative density function (CDF) of $\left| \mathbf{h}_{ij}^H \hat{\mathbf{w}}_i \right|^2$ given by

$$F(t) = \int_0^1 \left(f_1(x) \cdot f_2 \left(\frac{t}{x} \right) \right) dx. \quad (36)$$

Here,

$$f_1(x) = \frac{1}{\beta(1, N_C - 2)} (1 - x)^{N_C - 3}, \text{ for } 0 \leq x \leq 1, \quad (37)$$

$$f_2(x) = 1 - \text{etr}(-x\Sigma^{-1}) \sum_{k=0}^{N_T(N_C - N_T - 1)} \widehat{\sum}_{\kappa} \frac{C_{\kappa}(x\Sigma^{-1})}{k!}, \quad (38)$$

where $\beta(\cdot)$ is the beta function, $\kappa = (k_1, \dots, k_{N_T})$ denotes the partition of integer k with $k_1 \geq \dots \geq k_{N_T}$ and $k = k_1 + \dots + k_{N_T}$, $\text{etr}(\cdot)$ is $\exp(\text{tr}(\cdot))$, $\widehat{\sum}_{\kappa}$ denotes summation over the partitions $\kappa = (k_1, \dots, k_{N_T})$ of k with $k_1 \leq N_C - N_T - 1$, and $C_{\kappa}(\cdot)$ is the complex zonal polynomials (a.k.a. Schur polynomials). For $N_T = 2$ and $N_C = 3$, $F(t)$ is simplified as

$$F(t) = 1 - e^{-2t} + 2t \cdot \Gamma(0, 2t), \quad (39)$$

where $\Gamma(s, x) = \int_x^{\infty} t^{s-1} e^{-t} dt$ is the upper incomplete gamma function.

Proof. If we denote the PDF and CDF of $\left| \mathbf{h}_{ij}^H \hat{\mathbf{w}}_i \right|^2$ is denoted, $i, j \in \mathcal{N}_C$, by $f(t)$ and $F(t)$, respectively, the necessary condition for minimizing the MSQE is known as $y_j = \frac{\int_{b_{j-1}}^{b_j} t \cdot f(t) dt}{\int_{b_{j-1}}^{b_j} f(t) dt}$ [48], which can be modified as following via the integration by parts:

$$y_j = \frac{[-t(1 - F(t))]_{b_{j-1}}^{b_j} + \int_{b_{j-1}}^{b_j} (1 - F(t)) dt}{[F(t)]_{b_{j-1}}^{b_j}}. \quad (40)$$

Thus, (40) can be further simplified as (35).

The aim here is to derive the CDF $F(t)$. Since $\hat{\mathbf{w}}_i$ is obtained from (5) independently of \mathbf{h}_{ii} , $\forall i \in \mathcal{N}_C$, $\left| \mathbf{h}_{ii}^H \hat{\mathbf{w}}_i \right|^2$ is a chi-square random variable with degrees of freedom of 2. In case of $\left| \mathbf{h}_{ij}^H \hat{\mathbf{w}}_i \right|^2$, $i \neq j$, since $\hat{\mathbf{w}}_i$ is obtained as $\hat{\mathbf{w}}_i = \hat{\mathbf{v}}_i^{[N_T]}$, $\left| \mathbf{h}_{ij}^H \hat{\mathbf{w}}_i \right|^2 = 0$ if $(N_C - 1) < N_T$ and $\left| \mathbf{h}_{ij}^H \hat{\mathbf{w}}_i \right|^2 = \left(\hat{\sigma}_i^{[N_T]} \right)^2 \left| \hat{u}_i^{[j', N_T]} \right|^2$ otherwise, where $j' = j - 1$ if $i < j$ and $j' = j$ if $i > j$. Here, $\hat{\mathbf{v}}_i^{[N_T]}$ is the N_T -th column of the right singular matrix of $\hat{\mathbf{G}}_i$, $\hat{\sigma}_i^{[N_T]}$ is the N_T -th singular value of $\hat{\mathbf{G}}_i$, and $\hat{u}_i^{[j', N_T]}$ is the (j', N_T) -th element of the left singular matrix of $\hat{\mathbf{G}}_i$. If we define $\nu_i^{[N_T]}$ by $\nu_i^{[N_T]} = \left(\hat{\sigma}_i^{[N_T]} \right)^2$, the CDF of $\nu_i^{[N_T]}$ can be represented as f_2 in (38) [49]. If we define ξ_j by $\xi_j = \left| \hat{u}_i^{[j', N_T]} \right|^2$, the PDF of ξ_j is known as f_1 in (37) [50]. Since $\left(\hat{\sigma}_i^{[N_T]} \right)^2$ and $\left| \hat{u}_i^{[j', N_T]} \right|^2$ are independent, the CDF of $\left| \mathbf{h}_{ij}^H \hat{\mathbf{w}}_i \right|^2$, the product of $\left(\hat{\sigma}_i^{[N_T]} \right)^2$ and $\left| \hat{u}_i^{[j', N_T]} \right|^2$, can be represented as (36).

If $N_C - 1 = N_T$, the CDF of $\nu_i^{[N_T]}$ is simplified as [51]

$$f_2(x) = 1 - e^{-N_T x}. \quad (41)$$

Inserting (41) for $N_T = 2$ and $N_C = 3$ into (36) gives us (39). \square

Proposition 1. *Through integration by parts, the MSQE defined by $Q = \sum_{j=1}^M \int_{b_{j-1}}^{b_j} ((t - y_j)^2 \cdot f(t)) dt$, where $f(t)$ is the probability density function (PDF) of $\left| \mathbf{h}_{ij}^H \hat{\mathbf{w}}_i \right|^2$, can be written as a function of*

the CDF $F(t)$ as

$$Q = \sum_{j=1}^M \int_{b_{j-1}}^{b_j} 2(t - y_j)(1 - F(t))dt + \sum_{j=1}^M [-(t - y_j)^2(1 - F(t))]_{b_{j-1}}^{b_j}. \quad (42)$$

From Theorem 2 and Proposition 1, the Lloyd-Max algorithm minimizing the MSQE is obtained as Algorithm 1. Let n_f be the number of bits required to represent each quantized scalar information. Then, for given N_T and n_f , we define the codebook by \mathcal{K}_{N_T, n_f} which consists of 2^{n_f} elements. The codebooks designed by Algorithm 1 are shown in Table 1. For given codebook \mathcal{K}_{N_T, n_f} , the scalar value $|\mathbf{h}_{ij}^H \hat{\mathbf{w}}_i|^2$, $i, j \in \mathcal{N}_C$, to be shared by the BSs is quantized to $\psi_{ij}^{[N_T, n_f]}$ as follows:

$$\psi_{ij}^{[N_T, n_f]} = \arg \min_{\tau \in \mathcal{K}_{N_T, n_f}} \left| |\mathbf{h}_{ij}^H \hat{\mathbf{w}}_i|^2 - \tau \right|. \quad (43)$$

Algorithm 1 Iterative Lloyd-Max quantization algorithm

- 1) Set initial representative levels y_j for $j = 1, \dots, M$.
 - 2) Calculate decision thresholds $b_k = \frac{1}{2}(y_k + y_{k+1})$, for $k = 1, \dots, M - 1$.
 - 3) Calculate new representative levels y_j , $j = 1, \dots, M$, satisfying the necessary condition from (35).
 - 4) Repeat 2) and 3) until no further reduction in the MSQE Q given by (42).
-

Table 1: Codebooks designed by Algorithm 1

$\mathcal{K}_{2,1}$	{1.1936, 5.1831}
$\mathcal{K}_{2,2}$	{0.6693, 2.3922, 4.8012, 8.8195}
$\mathcal{K}_{2,3}$	{0.3559, 1.1559, 2.0747, 3.1561, 4.4735, 6.1395, 8.5331, 12.6185}
$\mathcal{K}_{4,1}$	{1.1779, 5.1301}
$\mathcal{K}_{4,2}$	{0.6540, 2.3447, 4.7196, 8.7581}
$\mathcal{K}_{4,3}$	{0.3471, 1.1306, 2.0333, 3.0925, 4.3799, 6.0385, 8.3822, 12.3984}

3.5 Backhaul Signaling Comparison

In this subsection, the amount of backhaul signaling required in the proposed scheme is compared to those of some existing schemes. The weighted minimizing mean-square error (WMMSE) scheme [44] maximizing the sum-rate is considered, where each beamforming vector is designed iteratively between the transmitters and receivers. It is known that the ‘WMMSE’ scheme is the most efficient scheme that achieves the optimal sum-rate bound iteratively but in a distributed manner. In the ‘WMMSE’ scheme, the vector information about beamforming vectors and the scalar information about receive equalizers and weight coefficients need to be exchanged between

the transmitters and receivers. The number of iteration in the ‘WMMSE’ scheme is denoted by π . The ‘Global’ scheme where all the beamforming vectors are jointly optimized in pursuit of maximizing the sum-rate [5] with the quantized channel vectors is also considered. For the optimal quantization of the channel vectors for the ‘Global’ scheme, the Grassmannian codebook is applied. Recall that the number of bits required for the quantization of each scalar value or vector by n_f . Table 2 summarizes the amount of required backhaul signaling in bits for the considered schemes. As shown in Table 2, the amount of the required backhaul signaling of the propose scheme is less than or equal to that of the ‘WMMSE’ scheme. Moreover, the required backhaul signaling of the ‘WMMSE’ scheme increases in proportion to the number of iteration π , which is shown by comparing the case of $N_C = 3$ and $\pi = 1$ and the case of $N_C = 3$ and $\pi = 2$.

Table 2: Amount of required backhaul signaling

Scheme		Proposed	WMMSE	Global	
Amount of backhaul signaling (in bits)	General	$n_f N_C^2 (N_C - 1)$	$3\pi n_f N_C^2$	$n_f N_C^2 (N_C - 1)$	
	$N_C = 3,$ $\pi = 1$	$n_f = 1$	18	27	18
		$n_f = 2$	36	54	36
		$n_f = 3$	54	81	54
	$N_C = 3,$ $\pi = 2$	$n_f = 1$	18	54	18
		$n_f = 2$	36	108	36
		$n_f = 3$	54	162	54
	$N_C = 7,$ $\pi = 2$	$n_f = 1$	294	294	294
		$n_f = 2$	588	588	588
		$n_f = 3$	882	882	882

3.6 Spectral Efficiency Comparison

Figures 2 and 3 demonstrate the average rates per cell versus SNR for the case of $N_T = 2$ and $N_C = 3$ and the case of and $N_T = 4$ and $N_C = 7$, respectively. The achievable sum-rate of the proposed scheme is evaluated under Rayleigh fading environment compared with other existing schemes. For the ‘WMMSE’ scheme, π is assumed to be 1 for $N_C = 3$ and 2 for $N_C = 7$ for fair comparison of the amount of the backhaul signaling. In addition, three schemes requiring only local CSI without information exchange are also considered as follows to show the impact of the exchanged information of the proposed scheme. First, the ‘Max-SNR’ scheme is considered, where all the beamforming vectors are designed only to maximize the desired signals. Second, the ‘Min-GI’ scheme [46] is considered, where all the beamforming vectors are determined only to minimize GI. Third, in the ‘Max-SLNR’ scheme [4], all the beamforming vectors are constructed maximizing SLNR. For the proposed scheme, the scalar quantization discussed in Section 3.4 with the codebook in Table 1 is used, whereas in the ‘WMMSE’ scheme, the Grassmannian codebook is applied for the beamforming vector quantization, and respective optimal scalar

quantization is applied for the quantization of the weight coefficients and receive equalizers. For the ‘Global’ scheme, the Grassmannian codebook is applied for the channel vector quantization and one bit is used for magnitude, whereas two bits are used for angle in cases of $n_f = 3$. As a baseline, ‘Random’ is considered, where each beamforming vector is randomly determined. For comparison, unquantized versions of the ‘WMMSE’ scheme and the proposed scheme are evaluated.

As seen in Figs. 2a and 3a, the ‘Max-SLNR’ scheme shows relatively high performance even without backhaul signaling. However, as the SNR increases, the proposed scheme shows notable rate gain compared with all the other schemes, in which each BS minimizes its GI signals with different weights designed improving the lower bound of the sum-rate. On the other hand, the sum of GI is minimized maximizing the desired channel gain in the ‘Max-SLNR’ scheme, which in general does not directly relate to the sum-rate for $N_C > 2$. With only $n_f = 3$, the proposed scheme already shows achievable rates close to its performance upper-bound, i.e., the achievable rate of the unquantized version of the proposed scheme. On the other hand, $n_f = 3$ are too small to quantize channel vectors, and hence the ‘Global’ scheme shows almost the same performance as the ‘Random’ scheme due to significant quantization error in the vector quantization. According to Table 2 and Figs. 2b and 3b, the rates of the proposed scheme with 18 bits ($N_C = 3$ and $n_f = 1$) of backhaul signaling and 294 bits ($N_C = 7$ and $n_f = 1$) of backhaul signaling are even higher than the rates of the ‘WMMSE’ scheme with 81 bits ($N_C = 3$ and $n_f = 3$) of backhaul signaling and 882 bits ($N_C = 7$ and $n_f = 3$) of backhaul signaling, respectively, in the SNR regime higher than 7dB for $N_C = 3$ and 9dB for $N_C = 7$, thereby improving the spectral efficiency and reducing the backhaul signaling at the same time.

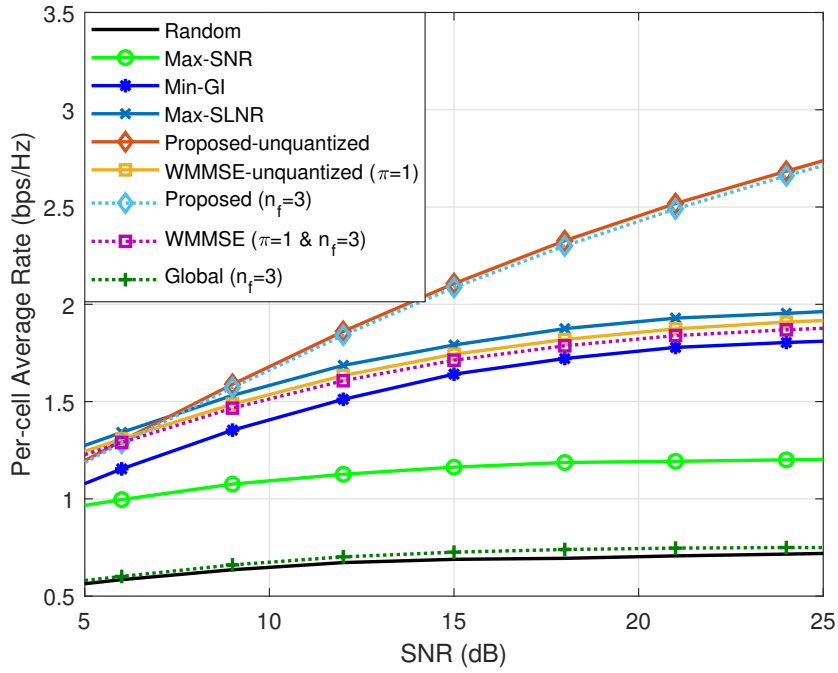
In Figs. 4 and 5, the average rate per cell of the proposed scheme versus SNR are compared with those of the existing schemes assuming antenna correlation between the transmit antennas. The Kronecker antenna correlation model [52] is used, and the antenna correlation matrices used for Figs. 4 and 5 are

$$\mathbf{R}_2 = \begin{bmatrix} 1 & 0.3 \\ 0.3 & 1 \end{bmatrix}, \quad (44)$$

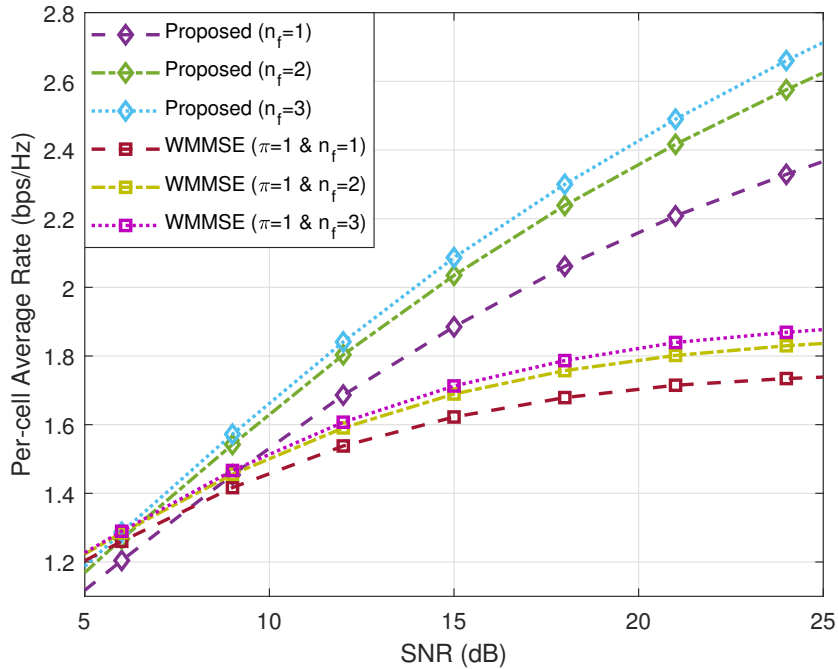
$$\mathbf{R}_4 = \begin{bmatrix} 1 & 0.3 & 0.3^2 & 0.3^3 \\ 0.3 & 1 & 0.3 & 0.3^2 \\ 0.3^2 & 0.3 & 1 & 0.3 \\ 0.3^3 & 0.3^2 & 0.3 & 1 \end{bmatrix}, \quad (45)$$

respectively. As shown in Figs. 4 and 5, the overall per-cell average rates of all the considered schemes are relatively degraded compared to those of Figs. 2a and 3a, respectively, due to the effect of the antenna correlation. However, the proposed scheme shows the maximum per-cell average rate in the SNR regime higher than 9dB and 12dB for the case of $N_T = 2$ and $N_C = 3$ and the case of $N_T = 4$ and $N_C = 7$, respectively. Moreover, the proposed scheme with $n_f = 3$ achieves the per-cell average rate which is close to that of the proposed scheme with unquantized

scalar information, labeled by 'Proposed-unquantized,' with only 3 bits of backhaul signaling for each scalar value.

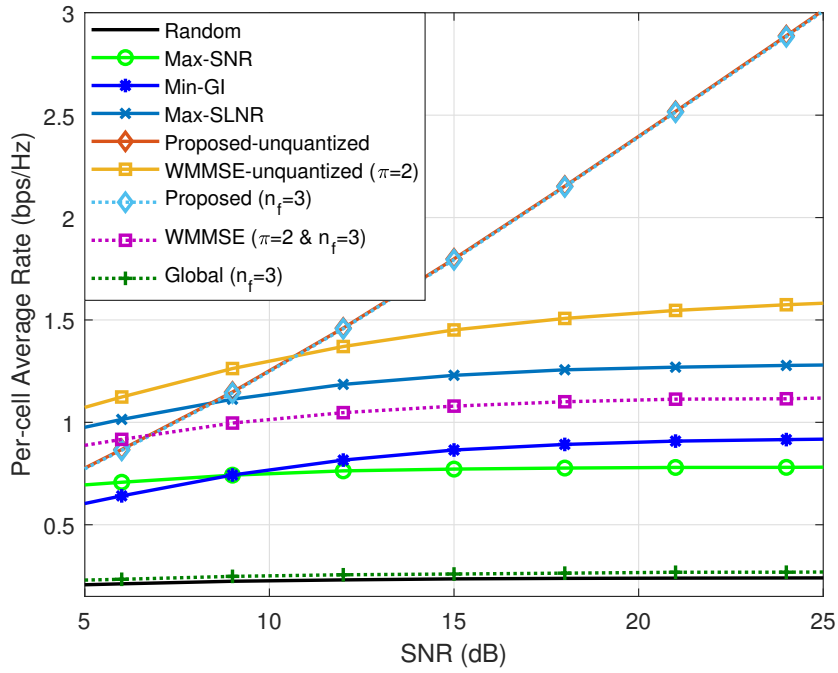


(a) Per-cell average rate versus SNR of the unquantized version of the proposed scheme compared to other existing scheme

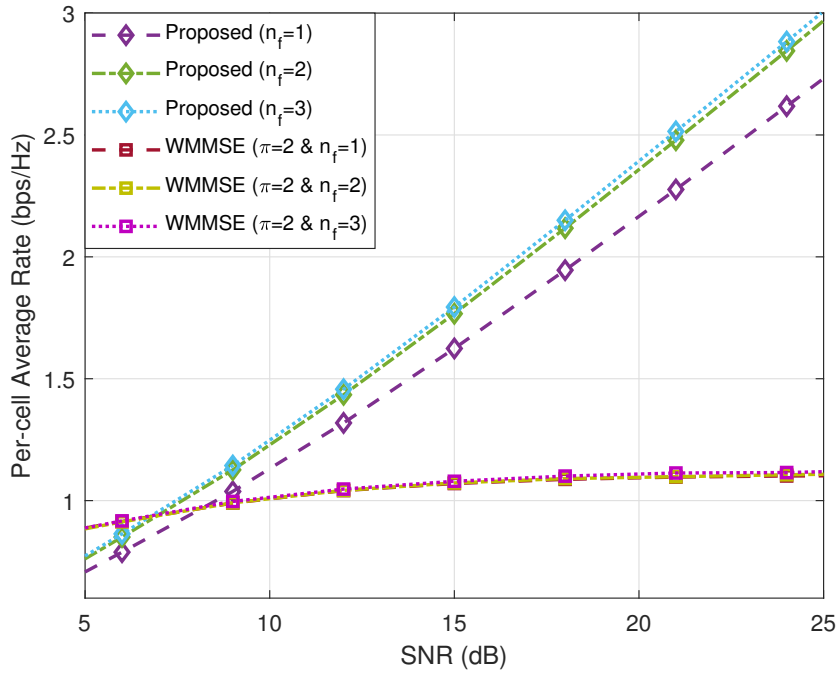


(b) Per-cell average rate versus SNR of the proposed scheme and the ‘WMMSE’ scheme for $n_f = 1, 2, 3$ and $\pi = 1$

Figure 2: Per-cell average rate versus SNR for $N_T = 2$ and $N_C = 3$



(a) Per-cell average rate versus SNR of the unquantized version of the proposed scheme compared to other existing scheme



(b) Per-cell average rate versus SNR of the proposed scheme and the ‘WMMSE’ scheme for $n_f = 1, 2, 3$ and $\pi = 2$

Figure 3: Per-cell average rate versus SNR for $N_T = 4$ and $N_C = 7$

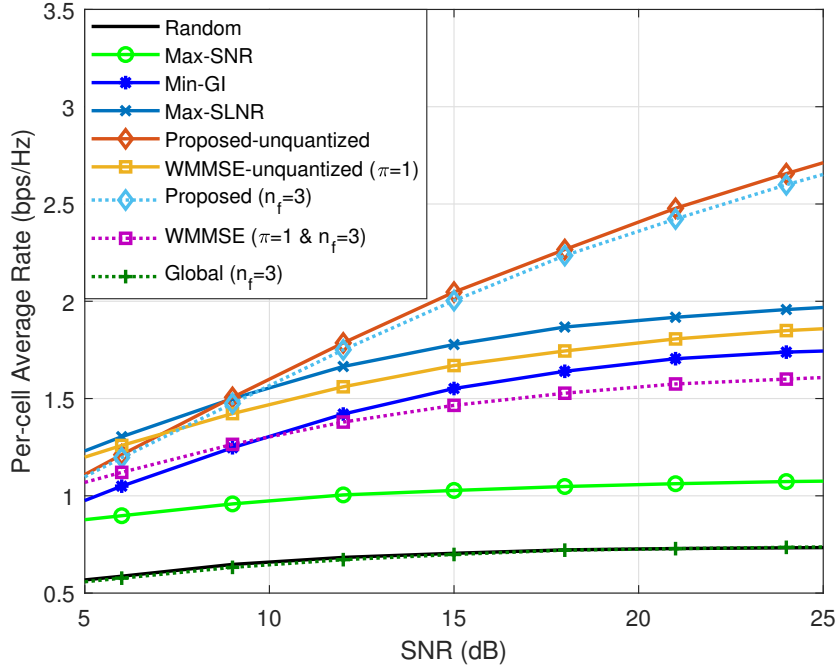


Figure 4: Per-cell average rate versus SNR for $N_T = 2$, $N_C = 3$, and the antenna correlation matrix \mathbf{R}_2

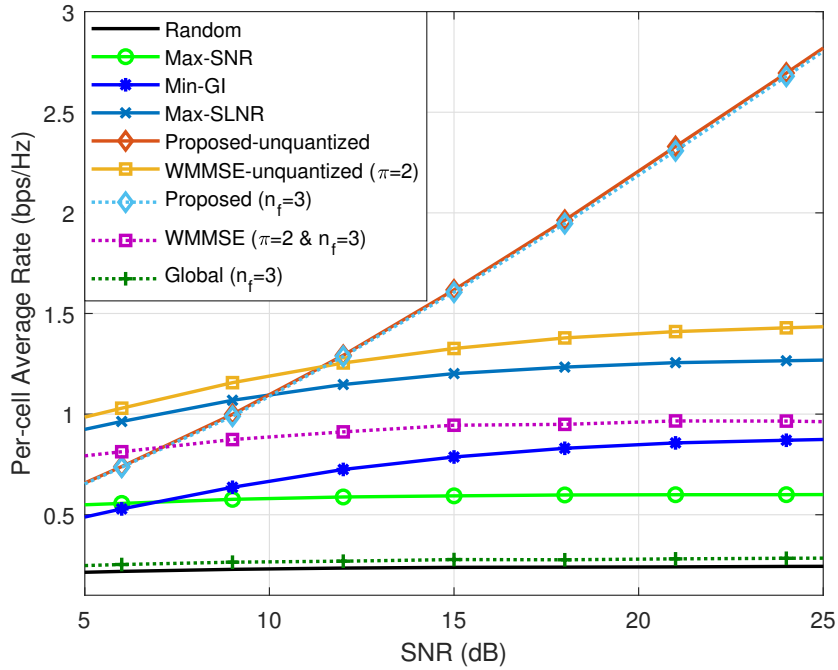


Figure 5: Per-cell average rate versus SNR for $N_T = 4$, $N_C = 7$, and the antenna correlation matrix \mathbf{R}_4

IV Proposed Beamforming Design 2 - Selection of IFUs

The sum-rate maximization problem should be formulated jointly for all the beamforming vectors as

$$(\mathbf{w}_1^*, \dots, \mathbf{w}_{N_C}^*) = \arg_{\mathbf{w}_1, \dots, \mathbf{w}_{N_C}} \max R(\mathbf{w}_1, \dots, \mathbf{w}_{N_C}), \text{ s.t. } \|\mathbf{w}_i\|^2 \leq 1, \forall i \in \mathcal{N}_C, \quad (46)$$

which requires global CSI to find the optimal solution. According to [4], the solution of the sum-rate maximization problem can also be obtained by solving the max-WSLNR problem. Specifically, let us denote the weight coefficient for the channel gain from BS i to user j by $\beta_{ij} \geq 0$, and the set of β_{ij} , $j \in \mathcal{N}_C$, by $\boldsymbol{\beta}_i = \{\beta_{i1}, \dots, \beta_{iN_C}\}$. Then, the beamforming vector in the max-WSLNR problem for given weights is obtained from

$$\mathbf{w}_{i, \boldsymbol{\beta}_i} = \arg_{\mathbf{w}_i, \|\mathbf{w}_i\|^2 \leq 1} \max \frac{\beta_{ii} |\mathbf{h}_{ii}^H \mathbf{w}_i|^2}{\sum_{j \in \mathcal{N}_C \setminus \{i\}} \beta_{ij} |\mathbf{h}_{ij}^H \mathbf{w}_i|^2 + N_0}. \quad (47)$$

Here, the weights should be jointly optimized to maximize the sum-rate as

$$(\boldsymbol{\beta}_1^*, \dots, \boldsymbol{\beta}_{N_C}^*) = \arg_{\boldsymbol{\beta}_1, \dots, \boldsymbol{\beta}_{N_C}} \max R(\mathbf{w}_{1, \boldsymbol{\beta}_1}, \dots, \mathbf{w}_{N_C, \boldsymbol{\beta}_{N_C}}). \quad (48)$$

The problems (47) and (48) are coupled with each other, and thus global CSI is required to solve these problems. To design the beamforming vectors with local CSI, in majority of the previous studies, all the weights are assumed to be identical, i.e., $\boldsymbol{\beta}_i = \mathbf{1}$, $\forall i \in \mathcal{N}_C$.

Our aim is to design $\boldsymbol{\beta}_i$, $i \in \mathcal{N}_C$, to maximize the sum-rate with local CSI and limited information exchange among the BSs. To gain intuition, we start with the following numerical example introducing the notion of *IFUs* (*IFUs*). If the received interference at user i , i.e., $\sum_{k \in \mathcal{N}_C \setminus \{i\}} |\mathbf{h}_{ki}^H \mathbf{w}_k|^2$ in (2), is significantly small, e.g., smaller than 1/100 of the maximum out of the interference strengths at all the users, then let us denote user i by an almost-interference-free user (almost-IFU). Figure 6 shows that the optimal per-cell average rate (left y-axis) and the average number of almost-IFUs (right y-axis) versus SNR for $N_T = 4$ and $N_C = 5$, where each channel is identically and independently distributed (i.i.d.) according to the complex Gaussian distribution. Here, the beamforming vectors are optimally designed through exhaustive numerical simulations based on global CSI. As shown in the figure, the average number of users with noticeably low interference increases from 0 to $N_T = 4$ as SNR increases. The lesson from Fig. 6 is that choosing a proper number of IFUs for given channel condition is essential to maximize the sum-rate. Indubitably, choosing a right set of IFUs, i.e., who shall be interfere-free, is also critical.

In what follows, we first propose a beamforming design framework based on the mixture of the WSLNR maximization and the WGI minimization for each possible number of IFUs. To

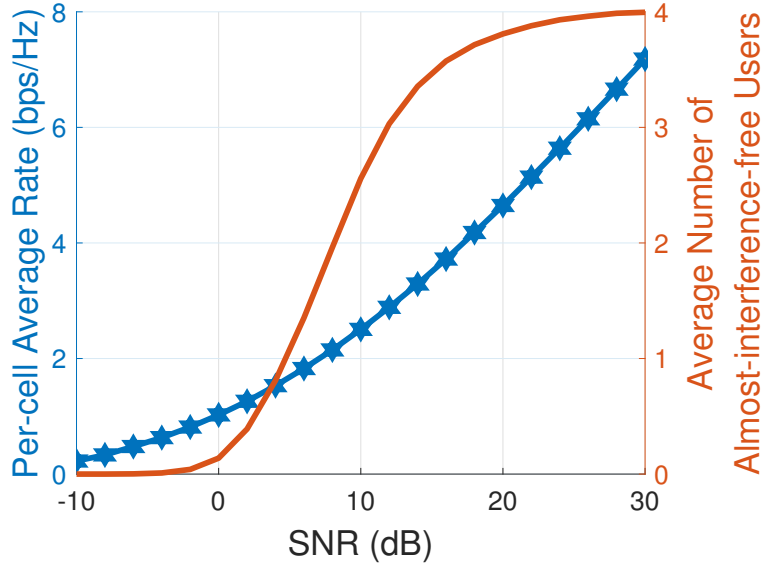


Figure 6: Average per-cell sum-rate and the average number of IFUs versus SNR for $N_T = 4$ and $N_C = 5$

begin, we define a general WSLNR in pursuit of incorporating the notion of WGI as

$$\chi_i = \begin{cases} \frac{\beta_{ii} |\mathbf{h}_{ii} \mathbf{w}_i|^2}{\sum_{j \in \mathcal{N}_C \setminus \{i\}} \beta_{ij} |\mathbf{h}_{ij} \mathbf{w}_i|^2 + N_0} & \text{if } \beta_{ii} \neq 0 \\ \frac{1}{\sum_{j \in \mathcal{N}_C \setminus \{i\}} \beta_{ij} |\mathbf{h}_{ij} \mathbf{w}_i|^2 + N_0} & \text{if } \beta_{ii} = 0, \end{cases} \quad (49)$$

where $\beta_{ij} \geq 0$ is the weight coefficient for the channel gain from BS i to user j . The essence of the proposed beamforming design is to restrict β_{ij} to $\beta_{ij} \in \{0, 1\}$ to work with limited information exchange among the BSs. The set of IFUs is denoted by \mathcal{F} , and the number of IFUs is denoted by α , i.e., $|\mathcal{F}| = \alpha$.

4.1 Beamforming vector design for $|\mathcal{F}| = N_T$

Assuming global CSI, the maximum multiplexing gain *without the time or frequency domain dimension extension* can be obtained by the interference alignment framework as summarized in the following proposition.

Proposition 2 (Theorem 1 in [53]). *With the interference alignment without dimension extension for the case of $N_C > N_T$, the maximum multiplexing gain is N_T .*

Proposition 2 implies that there can exist up to N_T users, the effective SINRs of which after proper receive processing incorporate zero inter-user interference, i.e., N_T IFUs. Since a single antenna at the receiver is assumed, no zero-forcing-like receive processing is possible. Thus, Proposition 2 in fact means that the SINRs of up to N_T users can be interfere-free only via transmit beamforming.

To shed light on obtaining N_T IFUs with local CSI, we introduce the following lemma.

Lemma 2. For $N_T < N_C$, given that each BS transmits with the equal power constraint $\|\mathbf{w}_i\|^2 = 1$, the optimal multiplexing gain of the multicell MISO downlink channel is $N_T - 1$ without time or frequency-domain signal extension.

Proof. Lemma 2 can be proved by following the similar footsteps of [53]. Note that the number of IFUs is $\alpha \leq N_C$, and hence the multiplexing gain is α . Suppose that user m is an IFU. Then, the interference-free constraints at the receiver side are given by

$$\mathbf{h}_{km}^H \mathbf{w}_k = 0, \quad k \in \mathcal{N}_C \setminus \{m\}. \quad (50)$$

The number of these equalities for the α IFUs is $\alpha(N_C - 1)$. On the other hand, the number of effective variables in each \mathbf{w}_n is $N_T - 1$ considering the unit-norm constraint. For the existence of the solution on \mathbf{w}_n of the equalities (50), we need the number of effective variables to be equal to or greater than the number of equalities, i.e., $\alpha(N_C - 1) \leq N_C(N_T - 1) \iff \alpha \leq \frac{N_C(N_T - 1)}{N_C - 1}$. Therefore, the maximum number of IFUs is given by

$$\alpha_{\max} = \left\lfloor \frac{N_C}{N_C - 1} (N_T - 1) \right\rfloor = N_T - 1 \quad (51)$$

for $N_C > N_T$, which proves the lemma. \square

Lemma 2 implies that the multiplexing gain of N_T cannot be obtained with the equal power constraint. Inspired by this fact, we notice that N_T IFUs can be obtained by employing $\|\mathbf{w}_k\|^2 = 0$ for some BSs, i.e., no effective transmission. The following lemma discusses the maximum number of IFUs based on this zero transmission power concept.

Lemma 3. The maximum number of IFUs in the MISO interference channel with $(N_C - N_A)$ BSs having zero transmission power is given by

$$\alpha_{\max} = \begin{cases} N_T & \text{if } N_A = N_T \\ N_T - 1 & \text{if } N_A > N_T \\ N_A & \text{otherwise,} \end{cases} \quad (52)$$

where N_A is the number of BSs with non-zero transmission power.

Proof. Note that the number of BSs with non-zero transmit power and the number of IFUs having non-zero strength of the desired signal are denoted as $N_A \leq N_C$ and $\alpha \leq N_A$, respectively. The condition on α can be obtained following the analogous footsteps of the proof of Lemma 2 by replacing N_C with N_A as $\alpha \leq \frac{N_A(N_T - 1)}{N_A - 1}$. Therefore, the maximum number of IFUs is given by

$$\alpha_{\max} = \left\lfloor \frac{N_A(N_T - 1)}{N_A - 1} \right\rfloor = \left\lfloor \frac{(N_A - 1)(N_T - 1) + N_T - 1}{N_A - 1} \right\rfloor. \quad (53)$$

Thus, choosing $N_A = N_T$, we have $\alpha_{\max} = N_T$. Note that $\alpha_{\max} = N_T - 1$ for $N_A > N_T$ and $\alpha_{\max} = N_A$ for $N_A < N_T$, which proves the lemma. \square

From Lemma 3, the maximum number of IFUs, N_T , can be obtained by simply muting $(N_C - N_T)$ BSs. In such a case, the index set of the active BSs with non-zero transmission power should be the same as the index set of the IFUs, denoted by \mathcal{F} . Specifically, the beamforming vectors are designed as follows. BS m for $m \in \mathcal{F}$ designs the beamforming vector that maximizes χ_m in (49) setting $\beta_{mm} = 0$ and $\beta_{mk} = 1$ for $k \in \mathcal{F} \setminus \{m\}$, and $\beta_{mn} = 0$ for $n \in \mathcal{N}_C \setminus \mathcal{F}$ as

$$\mathbf{w}_m^{\text{min-WGI}} = \arg \max_{\|\mathbf{w}\|^2=1} \frac{1}{\sum_{k \in \mathcal{F} \setminus \{m\}} |\mathbf{h}_{mk}^H \mathbf{w}|^2 + N_0} \quad (54)$$

$$= \arg \min_{\|\mathbf{w}\|^2=1} \|\mathbf{G}_m \mathbf{w}\|^2, \quad (55)$$

where $\mathbf{G}_m \triangleq [\sqrt{\beta_{m1}} \mathbf{h}_{m1}, \dots, \sqrt{\beta_{mN_C}} \mathbf{h}_{mN_C}]^H$. Then, the solution for the problem (54) is obtained by choosing the right singular vector of \mathbf{G}_m associated with the smallest singular value. Note that since we choose $\beta_{mm} = 0$ and $\beta_{mk} = 1$ for $k \in \mathcal{F} \setminus \{m\}$, and $\beta_{mn} = 0$ for $n \in \mathcal{N}_C \setminus \mathcal{F}$, the rank of \mathbf{G}_m is $(N_T - 1)$; that is, the smallest singular value is 0, yielding $\|\mathbf{G}_m \mathbf{w}_m^{\text{min-WGI}}\|^2 = 0$.

For $n \in \mathcal{N}_C \setminus \mathcal{F}$ and $\alpha = N_T$, we choose

$$\mathbf{w}_n = \mathbf{0}. \quad (56)$$

With this choice, the interference received at user m , $\forall m \in \mathcal{F}$, becomes zero, and the sum-rate is given by

$$R = \sum_{m \in \mathcal{F}} \log \left(1 + \frac{|\mathbf{h}_{mm}^H \mathbf{w}_m^{\text{min-WGI}}|^2}{N_0} \right). \quad (57)$$

It is crucial to design \mathcal{F} properly to maximize the sum-rate, which shall be obtained in Section 4.4.

Remark 2. *Turning off a set of base stations in small cell networks is used as one of the sum-rate improving technologies in 3GPP [18]. However, which and how many BSs should be turned off to maximize the sum-rate for given network has been investigated only empirically or heuristically. In this study, we derive which and how many BSs should be turned off in case of $|\mathcal{F}| = N_T$ to nearly achieve the maximum capacity bound.*

4.2 Beamforming vector design for $|\mathcal{F}| = N_T - 1$

From Lemma 3, $|\mathcal{F}| = \alpha = N_T - 1$ can be obtained by having $N_A \geq N_T - 1$. Setting N_A to its maximum value, i.e., $N_A = N_C$, does not harm the sum-rate because more non-zero rates from BS n , $n \in \mathcal{N}_C \setminus \mathcal{F}$, are added in the sum-rate than with $N_A < N_C$. Thus, for $\alpha = N_T - 1$, we choose to set $N_A = N_C$. For $\alpha = N_T - 1$, we consider the following beamforming designs with local CSI.

4.2.1 BS n for $n \in \mathcal{N}_C \setminus \mathcal{F}$

Note that each beamforming vector of size N_T has null space size of $N_T - 1$. Thus, to make user m , $m \in \mathcal{F}$, interference-free, BS n , $n \in \mathcal{N}_C \setminus \mathcal{F}$ should employ the min-WGI beamforming design in (54) as follows:

$$\mathbf{w}_n^{\text{min-WGI}} = \arg \min_{\|\mathbf{w}\|^2=1} \sum_{m \in \mathcal{F}} |\mathbf{h}_{nm}^H \mathbf{w}|^2. \quad (58)$$

4.2.2 BS m for $m \in \mathcal{F}$

Since BS m for $m \in \mathcal{F}$ only needs to make zero interference to the BSs with the indices in $\mathcal{F} \setminus \{m\}$, where $|\mathcal{F} \setminus \{m\}| = N_T - 2$, BS m can utilize the space of rank one either to improve the desired channel gain or to make zero-interference to user l for $l \in \mathcal{N}_C \setminus \mathcal{F}$. Specifically, to make zero-interference to user l for $l \in \mathcal{N}_C \setminus \mathcal{F}$, BS m for $m \in \mathcal{F}$ would set $\beta_{mq} = 1$ for $q \in (\mathcal{F} \cup \{l\}) \setminus \{m\}$ and $\beta_{mm} = \beta_{mn} = 0$ for $n \in \mathcal{N}_C \setminus \mathcal{F}$ and design its beamforming vector maximizing (49) from

$$\mathbf{w}_m^{\text{min-WGI}} = \arg \min_{\|\mathbf{w}\|^2=1} \sum_{q \in (\mathcal{F} \cup \{l\}) \setminus \{m\}} |\mathbf{h}_{mq}^H \mathbf{w}|^2. \quad (59)$$

On the other hand, to improve the desired channel gain, BS m for $m \in \mathcal{F}$ would set $\beta_{mm} = \beta_{mk} = 1$ for $k \in \mathcal{F} \setminus \{m\}$ and $\beta_{mn} = 0$ for $n \in \mathcal{N}_C \setminus \mathcal{F}$ and design its beamforming vector maximizing (49) as

$$\mathbf{w}_m^{\text{max-WSLNR}} = \arg \max_{\|\mathbf{w}\|^2=1} \frac{|\mathbf{h}_{mm}^H \mathbf{w}|^2}{\sum_{k \in \mathcal{F} \setminus \{m\}} |\mathbf{h}_{mk}^H \mathbf{w}|^2 + N_0} \quad (60)$$

$$= \arg \max_{\|\mathbf{w}\|^2=1} \frac{\mathbf{w}^H \mathbf{A}_m \mathbf{w}}{\mathbf{w}^H \mathbf{B}_m \mathbf{w}}, \quad (61)$$

where $\mathbf{A}_m = \mathbf{h}_{mm} \mathbf{h}_{mm}^H$ and $\mathbf{B}_m = \sum_{k \in \mathcal{F} \setminus \{m\}} \mathbf{h}_{mk} \mathbf{h}_{mk}^H + N_0 \mathbf{I}$. Then, the solution of (60) is given

by the eigenvector of $\mathbf{B}_m^{-1} \mathbf{A}_m$ associated with the maximum eigenvalue.

To discuss the difference between the aforementioned two strategies in the sense of maximizing the sum-rate, we establish the following theorem.

Theorem 3. For BS m , $m \in \mathcal{F}$, and $\alpha = N_T - 1$, let us denote the sum-rate for the case (referred to as Case 1) where BS m employs the max-WSLNR beamforming from (60) as R_1 , and the sum-rate for the case (referred to as Case 2) where BS m employs the min-WGI beamforming from (59) by R_2 . For both the cases, BS n , $n \in \mathcal{N}_C \setminus \mathcal{F}$, designs its beamforming vector from (58). Then, we have $R_1 - R_2 \geq 0$ in low- and high-SNR regime.

Proof. The sum-rate for Case 1, R_1 , can be represented as

$$R_1 = \sum_{m \in \mathcal{F}} \log \left(1 + \frac{\tilde{\eta}_{mm}^{[1]}}{N_0} \right) + \sum_{n \in \mathcal{N}_C \setminus \mathcal{F}} \log \left(1 + \frac{\tilde{\eta}_{nn}^{[2]}}{\sum_{m \in \mathcal{F}} \tilde{\eta}_{mn}^{[1]} + \sum_{v \in \mathcal{N}_C \setminus \mathcal{F}, v \neq n} \tilde{\eta}_{vn}^{[2]} + N_0} \right), \quad (62)$$

where $\tilde{\eta}_{ij}^{[1]} = \left| \mathbf{h}_{ij}^H \mathbf{w}_i^{\max\text{-WSLNR}} \right|^2$ and $\tilde{\eta}_{ij}^{[2]} = \left| \mathbf{h}_{ij}^H \mathbf{w}_i^{\min\text{-WGI}} \right|^2$.

To compute R_2 , suppose that BSs $m, m \in \mathcal{F}$, make GI to another user $l, l \in \mathcal{N}_C \setminus \mathcal{F}$, zero.

Then, R_2 can be represented as

$$R_2 = \sum_{m \in \mathcal{F}} \log \left(1 + \frac{\tilde{\eta}_{mm}^{[2]}}{N_0} \right) + \log \left(1 + \frac{\tilde{\eta}_{ll}^{[2]}}{\sum_{g \in \mathcal{N}_C \setminus \mathcal{F}, g \neq l} \tilde{\eta}_{gl}^{[2]} + N_0} \right) + \sum_{n \in \mathcal{N}_C \setminus \mathcal{F}, n \neq l} \log \left(1 + \frac{\tilde{\eta}_{mn}^{[2]}}{\sum_{h \in \mathcal{N}_C \setminus \{n\}} \tilde{\eta}_{hn}^{[2]} + N_0} \right). \quad (63)$$

i) In low-SNR regime, i.e., N_0 is arbitrarily large,

$$R_1 \simeq \sum_{m \in \mathcal{F}} \log \left(1 + \frac{\tilde{\eta}_{mm}^{[1]}}{N_0} \right) + \sum_{n \in \mathcal{N}_C \setminus \mathcal{F}_c} \log \left(1 + \frac{\tilde{\eta}_{mn}^{[2]}}{N_0} \right), \quad (64)$$

$$R_2 \simeq \sum_{m \in \mathcal{F}} \log \left(1 + \frac{\tilde{\eta}_{mm}^{[2]}}{N_0} \right) + \sum_{n \in \mathcal{N}_C \setminus \mathcal{F}} \log \left(1 + \frac{\tilde{\eta}_{mn}^{[2]}}{N_0} \right). \quad (65)$$

Consequently, we have

$$R_1 - R_2 \simeq \sum_{m \in \mathcal{F}} \log \left(1 + \frac{\tilde{\eta}_{mm}^{[1]}}{N_0} \right) - \sum_{m \in \mathcal{F}} \log \left(1 + \frac{\tilde{\eta}_{mm}^{[2]}}{N_0} \right), \quad (66)$$

$$\simeq \sum_{m \in \mathcal{F}} \log \left(1 + \frac{\|\mathbf{h}_{mm}\|^2}{N_0} \right) - \sum_{m \in \mathcal{F}} \log \left(1 + \frac{\tilde{\eta}_{mm}^{[2]}}{N_0} \right), \quad (67)$$

where (67) follows from the fact that the max-WSLNR problem (60) becomes the max-SNR problem for arbitrarily large N_0 , yielding $\tilde{\eta}_{mm}^{[1]} = \left| \mathbf{h}_{mm}^H \mathbf{w}_m^{\max\text{-WSLNR}} \right|^2 \simeq \|\mathbf{h}_{mm}\|^2$. Since $\|\mathbf{h}_{mm}\|^2 \geq \left| \mathbf{h}_{mm}^H \mathbf{w} \right|^2$ for any unit-norm \mathbf{w} , we have $\|\mathbf{h}_{mm}\|^2 \geq \tilde{\eta}_{mm}^{[2]}$ for $m \in \mathcal{F}$, which proves the theorem for low-SNR regime.

ii) In high-SNR regime, i.e., N_0 is arbitrarily small, the achievable rates of the IFUs, which have zero interference, are dominant due to the interference terms in the achievable rates of the other users. Thus, we have $R_1 \simeq \sum_{m \in \mathcal{F}_c} \log \left(1 + \frac{\tilde{\eta}_{mm}^{[1]}}{N_0} \right)$ and $R_2 \simeq \sum_{m \in \mathcal{F}_c} \log \left(1 + \frac{\tilde{\eta}_{mm}^{[2]}}{N_0} \right)$, and hence, we again have the same $R_1 - R_2$ expression as in (66). In Case 1, \mathbf{w}_m for $m \in \mathcal{F}$ is designed to have the direction of the orthogonal projection of \mathbf{h}_{mm} onto the null space of \mathbf{h}_{mn} , $n \in \mathcal{F} \setminus \{m\}$. On the other hand, in Case 2, the beamforming vector is designed to have the direction of the null space of \mathbf{h}_{mn} and \mathbf{h}_{ml} . That is, the beamforming vector is designed independently of \mathbf{h}_{mm} on the null space of \mathbf{h}_{mn} , $n \in \mathcal{F} \setminus \{m\}$. Therefore, we have

$$\tilde{\eta}_{mm}^{[1]} = \left| \mathbf{h}_{mm}^H \mathbf{w}_m^{\max\text{-WSLNR}} \right|^2 \geq \tilde{\eta}_{mm}^{[2]} = \left| \mathbf{h}_{mm}^H \mathbf{w}_m^{\min\text{-WGI}} \right|^2, \quad (68)$$

which proves the theorem for high-SNR regime. \square

From Theorem 3, we propose to design \mathbf{w}_m for $\alpha = N_T - 1$, $m \in \mathcal{F}$, from the max-WSLNR problem of (60). The sum-rate with such a choice is given by (69).

$$\begin{aligned}
R = & \underbrace{\sum_{m \in \mathcal{F}} \log \left(1 + \frac{|\mathbf{h}_{mm}^H \mathbf{w}_m^{\max\text{-WSLNR}}|^2}{N_0} \right)}_{\text{no received interference}} \\
& + \underbrace{\sum_{n \in \mathcal{N}_C \setminus \mathcal{F}} \log \left(1 + \frac{|\mathbf{h}_{nn}^H \mathbf{w}_n^{\min\text{-WGI}}|^2}{\sum_{m \in \mathcal{F}} |\mathbf{h}_{mn}^H \mathbf{w}_m^{\max\text{-WSLNR}}|^2 + \sum_{v \in \mathcal{N}_C \setminus \mathcal{F}, v \neq n} |\mathbf{h}_{vn}^H \mathbf{w}_v^{\min\text{-WGI}}|^2 + N_0} \right)}_{\text{includes interference received from all the BSs}} \quad (69)
\end{aligned}$$

Again, the design of \mathcal{F} shall be provided in Section 4.4.

4.3 Beamforming vector design for $|\mathcal{F}| \leq N_T - 2$

For $|\mathcal{F}| = \alpha \leq N_T - 2$, all the BSs design their beamforming vectors making zero GI to user m , $m \in \mathcal{F}$. The number of neighboring users, to which each BS makes GI zero, is $\alpha - 1$ for BS m , $m \in \mathcal{F}$, and α for BS n , $n \in \mathcal{N}_C \setminus \mathcal{F}$. That is, BS m , $m \in \mathcal{F}$, designs its beamforming vector maximizing the desired channel gain and making GI zero to user k , $k \in \mathcal{F} \setminus \{m\}$, and BS n , $n \in \mathcal{N}_C \setminus \mathcal{F}$, designs its beamforming vectors maximizing the desired channel gain and making GI zero to user m , $m \in \mathcal{F}$. Then, the beamforming vectors of BS m and BS n are designed in the null spaces of ranks $(N_T - \alpha + 1)$ and $(N_T - \alpha)$, respectively. Then, for $\alpha \leq N_T - 2$, all the beamforming vectors are obtained from the max-WSLNR problem of (60). The sum-rate in such a case is given by

$$\begin{aligned}
R = & \underbrace{\sum_{m \in \mathcal{F}} \log \left(1 + \frac{|\mathbf{h}_{mm}^H \mathbf{w}_m^{\max\text{-WSLNR}}|^2}{N_0} \right)}_{\text{no received interference}} + \underbrace{\sum_{n \in \mathcal{N}_C \setminus \mathcal{F}} \log \left(1 + \frac{|\mathbf{h}_{nn}^H \mathbf{w}_n^{\max\text{-WSLNR}}|^2}{\sum_{h \in \mathcal{N}_C \setminus \{n\}} |\mathbf{h}_{hn}^H \mathbf{w}_h^{\max\text{-WSLNR}}|^2 + N_0} \right)}_{\text{includes interference received from all the BSs}}. \quad (70)
\end{aligned}$$

The examples of the beamforming vector design protocol with $N_T = 4$ and $N_C = 7$ for $\alpha = N_T = 4$, $\alpha = N_T - 1 = 3$, and $\alpha = N_T - 2 = 2$ are illustrated in Figs. 7a, 7b, and 7c, respectively.

4.4 Selection of \mathcal{F} : Design of β_{ij}

Now, the aim is to determine a proper number of IFUs, α , and the set of IFUs, \mathcal{F} , out of all possible cases in pursuit of maximizing the sum-rate with local CSI and limited information exchange. Totally, there exist $N_K = \binom{N_C}{N_T} + \binom{N_C}{N_T-1} + \dots + \binom{N_C}{1}$ possible IFUs selection.

Let us denote the c -th IFU selection, $c \in \{1, \dots, N_K\}$, by \mathcal{F}_c , i.e., users m , $m \in \mathcal{F}_c$, have received interference of zero. With this IFUs selection of \mathcal{F}_c , the rate of user i is denoted by $r_i^{[c]}$ and the beamforming vector of BS i is denoted by $\mathbf{w}_i^{[c]}$. Then, the sum-rate for the c -th IFU

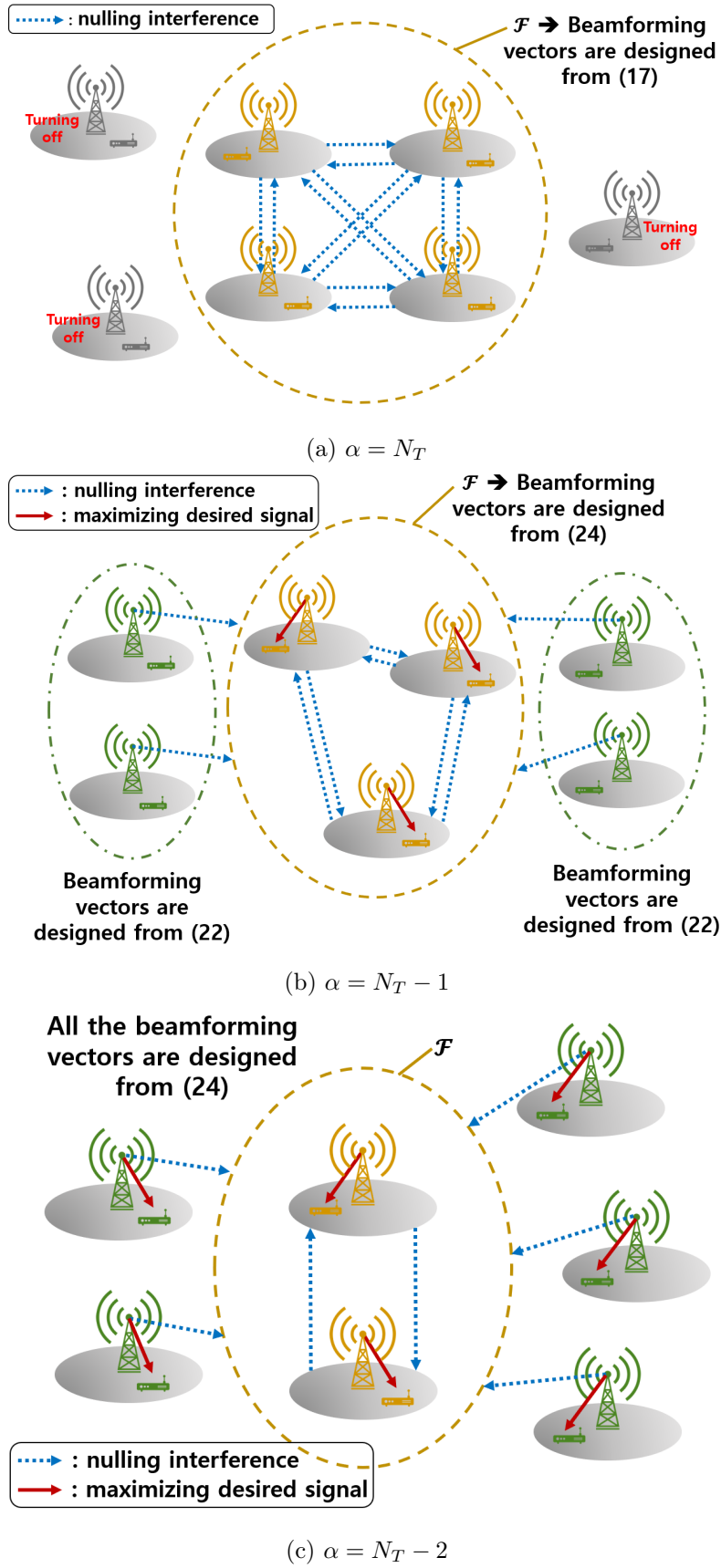


Figure 7: Illustration of the proposed multicell beamforming vector design

selection can be represented as

$$R^{[c]} = \underbrace{\sum_{m \in \mathcal{F}_c} \log \left(1 + \frac{\eta_{mm}^{[c]}}{N_0} \right)}_{\triangleq R_{\text{local}}^{[c]}} + \underbrace{\sum_{n \in \mathcal{N}_C \setminus \mathcal{F}_c} \log \left(1 + \frac{\eta_{nn}^{[c]}}{T_n^{[c]}} \right)}_{\triangleq R_{\text{global}}^{[c]}}, \quad (71)$$

where $\eta_{ij}^{[c]} = \left| \mathbf{h}_{ij}^H \mathbf{w}_i^{[c]} \right|^2$ and $T_n^{[c]} = \sum_{k \in \mathcal{N}_C \setminus \{n\}} \eta_{kn}^{[c]} + N_0$. Herein, the first term $R_{\text{local}}^{[c]}$ is the sum of rates of user m , $m \in \mathcal{F}_c$, which can be computed with only local CSI by BS m . On the other hand, the second term $R_{\text{global}}^{[c]}$ is the sum of rates of user n which require global CSI to be computed by BS n , $n \in \mathcal{N}_C \setminus \mathcal{F}_c$.

For $\alpha = N_T$, $R_{\text{global}}^{[c]}$ is zero since BS n , $n \in \mathcal{N}_C \setminus \mathcal{F}$, has zero transmit power. Therefore, we have $R^{[c]} = R_{\text{local}}^{[c]}$ and it requires only local CSI to be available at BS m , $m \in \mathcal{F}_c$. However, for $\alpha \leq N_T - 1$, $R_{\text{global}}^{[c]}$ is non-zero and requires global CSI to be available at all the BSs. Thus, we propose to consider the upper bound of the average $R_{\text{global}}^{[c]}$ which can be computed at all the BSs with only local CSI. To get the upper bound of $E\{R_{\text{global}}^{[c]}\}$ for $\alpha \leq N_T - 1$, we establish the following lemma.

Lemma 4. For all $c \in \{1, \dots, N_K\}$ and $\alpha \leq N_T - 1$,

$$E\{R_{\text{global}}^{[c]}\} \leq \bar{R}_{\text{global}}^{[c]} = (N_C - \alpha) \log \left(1 + \frac{(N_T - \alpha)e^{\frac{N_0}{2}}}{\left(\frac{N_0}{2}\right)^{2-N_C}} \Gamma \left(2 - N_C, \frac{N_0}{2} \right) \right), \quad (72)$$

where $\Gamma(s, t) = \int_t^\infty x^{s-1} e^{-x} dx$ is the incomplete gamma function.

Proof. for $\alpha \leq N_T - 1$, the expectation of $R_{\text{global}}^{[c]}$ can be bounded as follows:

$$E\{R_{\text{global}}^{[c]}\} = E \left\{ \sum_{n \in \mathcal{N}_C \setminus \mathcal{F}_c} \log \left(1 + \eta_{nn}^{[c]} / T_n^{[c]} \right) \right\} \quad (73)$$

$$\leq \sum_{n \in \mathcal{N}_C \setminus \mathcal{F}_c} \log \left(1 + E\{\eta_{nn}^{[c]}\} E\{1/T_n^{[c]}\} \right). \quad (74)$$

i) $E\{\eta_{nn}^{[c]}\}$, $n \in \mathcal{N}_C \setminus \mathcal{F}_c$: For $\alpha = N_T - 1$, $\mathbf{w}_n^{[c]}$ is designed independently with \mathbf{h}_{nm} , and hence, $\eta_{nn}^{[c]} = \left| \mathbf{h}_{nn}^H \mathbf{w}_n^{[c]} \right|^2$ is a Chi-square random variable with degrees of freedom (DoF) 2. On the other hand, for $\alpha \leq N_T - 2$, $\mathbf{w}_n^{[c]}$ lies in the orthogonal projection of \mathbf{h}_{nn} onto the null space of \mathbf{h}_{nm} , $m \in \mathcal{F}_c$. Let us denote \mathbf{b}_p as the p -th basis vector of the null space of \mathbf{h}_{nm} . The rank of the space composed of these basis vectors is $(N_T - \alpha)$. Then, the desired channel gain can be represented as

$$\left| \mathbf{h}_{nn}^H \mathbf{w}_n^{[c]} \right|^2 = \left\| \sum_{p=1}^{N_T - \alpha} |\mathbf{h}_{nn} \mathbf{b}_p| \cdot \mathbf{b}_p \right\|^2 = \sum_{p=1}^{N_T - \alpha} |\mathbf{h}_{nn} \mathbf{b}_p|^2, \quad (75)$$

and it is a Chi-square random variable with DoF of $2(N_T - \alpha)$ which is 2 for $\alpha = N_T - 1$. Thus, we get $E\{\eta_{nn}^{[c]}\} = 2(N_T - \alpha)$ for $\alpha \leq N_T - 1$.

ii) $E\left\{1/T_n^{[c]}\right\}$, $n \in \mathcal{N}_C \setminus \mathcal{F}_c$: For $\alpha \leq N_T - 1$, $\mathbf{w}_k^{[c]}$, $k \in \mathcal{N}_C \setminus \{n\}$, is designed independently with \mathbf{h}_{kn} . Thus, $\eta_{kn}^{[c]} = \left|\mathbf{h}_{kn}^H \mathbf{w}_k^{[c]}\right|^2$ is a Chi-square random variable with DoF 2. Then, we get

$$E\left\{1/T_n^{[c]}\right\} = e^{\frac{N_0}{2}} \cdot 2^{1-N_C} \cdot N_0^{N_C-2} \cdot \Gamma(2 - N_C, N_0/2), \quad (76)$$

where $\Gamma(s) = (s - 1)!$ is the gamma function.

From the above two results, the expectation of $R_{\text{global}}^{[c]}$ for $\alpha \leq N_T - 1$ can be further bounded as follows:

$$E\left\{R_{\text{global}}^{[c]}\right\} \leq (N_C - \alpha) \log\left(1 + \frac{(N_T - \alpha)\Gamma(2 - N_C, \frac{N_0}{2})}{e^{-\frac{N_0}{2}} \left(\frac{N_0}{2}\right)^{2-N_C}}\right), \quad (77)$$

which proves the lemma. \square

From Lemma 4, we propose to select the index set \mathcal{F} for $\alpha \leq N_T - 1$, which maximizes $R_{\text{local}}^{[c]} + \bar{R}_{\text{global}}^{[c]}$. Note that $\bar{R}_{\text{global}}^{[c]} = 0$ for $|\mathcal{F}| = \alpha = N_T$, and hence the cost function $R_{\text{local}}^{[c]} + \bar{R}_{\text{global}}^{[c]}$ can be used for all possible α values discussed. At this point, to compromise between the amount of information exchange among BSs and the sum-rate performance, let us assume that the information of $r_m^{[c]}$, $m \in \mathcal{F}_c$, is collected only for the cases with selected α . In this case, let us denote the set of considered α and the index set of the considered cases as \mathcal{A} and \mathcal{N}_G , respectively. If the set of considered α is $\mathcal{A} = \{N_T - 2, N_T\}$ for $N_T = 3$ and $N_C = 4$, we have $|\mathcal{N}_G| = \binom{N_C}{N_T} + \binom{N_C}{N_T-2} = 8$. Then, the index set \mathcal{F} optimization problem is formulated as

$$\mathcal{F} = \mathcal{F}_{c^*}, \quad (78)$$

where

$$c^* = \arg \max_{c \in \mathcal{N}_G} R_{\text{local}}^{[c]} + \bar{R}_{\text{global}}^{[c]}. \quad (79)$$

4.4.1 Tightness of the upper bound $\bar{R}_{\text{global}}^{[c]}$

The gap of $E\{R_{\text{global}}^{[c]}\}$ and $\bar{R}_{\text{global}}^{[c]}$ results only from the Jensen's inequality in (74). The analysis of Jensen's gap has been extensively studied in the literature [54, 55]. The gap in the inequality (74) tends to 0 if the random variable $X_n = 1 + \eta_{nn}^{[c]}/T_n^{[c]}$ is almost surely constant. The bound of the gap in case where X_n is mean-centric is derived in [55]. In addition, the log function becomes an affine function for small X_n , resulting in the gap tending to 0. In summary, as received interference at user n , $n \in \mathcal{N}_C \setminus \mathcal{F}$, becomes significantly stronger than the desired signal gain, the gap in (72) tends to zero. Furthermore, the more the SINR X_n becomes mean-centric, the tighter upper bound we can get from (72).

4.4.2 Asymptotic performance of using $\bar{R}_{\text{global}}^{[c]}$

In the high SNR regime, i.e., N_0 is arbitrarily small, $R_{\text{local}}^{[c]}$ becomes dominant in (71) and we have $R^{[c]} = R_{\text{local}}^{[c]} + R_{\text{global}}^{[c]} \simeq R_{\text{local}}^{[c]}$, for all $c \in \{1, \dots, N_K\}$. In addition, $\bar{R}_{\text{global}}^{[c]}$ also tends to 0 in the high SNR regime. Therefore, the proposed design is asymptotically optimal as SNR

increases. In finite SNR regime, as α grows for fixed N_C , $R_{\text{local}}^{[c]}$ in (71) becomes dominant since the number of rate terms in $R_{\text{global}}^{[c]}$ which require global CSI, $(N_C - \alpha)$, decreases. On the other hand, as N_C increases for fixed α , the number of interference terms $\eta_{kn}^{[c]}$ in $R_{\text{global}}^{[c]}$ increases, and the number of rate terms in $R_{\text{global}}^{[c]}$ also increases. It can be readily shown that this global CSI term tends to be bounded by a constant value even in the high-SNR regime, following the analysis in [3]. Hence, for high-SNR regime, where the $R_{\text{local}}^{[c]}$ terms tend to be infinite, or for large α compared with N_C , the global CSI terms $R_{\text{global}}^{[c]}$ become negligible compared to the local CSI terms, resulting in $\bar{R}_{\text{global}}^{[c]}$ also tending to 0.

4.4.3 Performance of using $\bar{R}_{\text{global}}^{[c]}$ in finite SNR, N_T , and N_C

Figure 10 shows the per-cell average $R_{\text{global}}^{[c]}$ and $\bar{R}_{\text{global}}^{[c]}$ versus SNR for $N_T = 4$ and $N_C = 7$, where each channel is i.i.d. according to the complex Gaussian distribution. As shown in this figure, the gap between $\text{E}\{R_{\text{global}}^{[c]}\}$ and $\bar{R}_{\text{global}}^{[c]}$ is smaller than 0.04bps/Hz for all possible α values, showing that $\bar{R}_{\text{global}}^{[c]}$ is a good estimator of $\text{E}\{R_{\text{global}}^{[c]}\}$ even with finite parameter values.

4.5 Information exchange

To compute the cost function of the problem (79), $R_{\text{local}}^{[c]} + \bar{R}_{\text{global}}^{[c]}$, each rate term of $R_{\text{local}}^{[c]}$, $\log\left(1 + \eta_{mm}^{[c]}/N_0\right)$, needs to be computed by BS m , $m \in \mathcal{F}_c$, with local CSI and be shared by all the BSs. The term $\bar{R}_{\text{global}}^{[c]}$ can be computed by any BS without any extra information on instantaneous channels. Let us denote the rate of user m for $m \in \mathcal{F}_c$ with the c -th IFU selection by

$$r_m^{[c]} = \log\left(1 + \eta_{mm}^{[c]}/N_0\right). \quad (80)$$

An example case is as shown in Table 3, where $N_T = 3$, $N_C = 4$, and $\mathcal{A} = \{N_T - 2, N_T\}$. Here, BS 1 can compute the achievable rates in the white cells of the column of BS 1 with only local CSI and does not compute the achievable rates correspond to the dark gray cells in the column of BS 1 in Table 3, because they require global CSI to be computed. Though each BS can compute $\binom{3}{2} + \binom{3}{1} + \binom{3}{0} = 7$ rate terms with local CSI, BS m shares $r_m^{[c]}$ values only for $c \in \mathcal{N}_G$ to restrict the amount of information exchange. Then, for given c , $c \in \mathcal{N}_G$, $R_{\text{local}}^{[c]}$ is computed by adding all the collected rate terms, i.e., collected rate terms in each row of Table 3, the problem (79) can be formulated together with $\bar{R}_{\text{global}}^{[c]}$.

4.6 Quantization optimization

In this subsection, the quantization of rate terms that need to be exchanged is analyzed, which is crucial to exchange the information with finite bits. Let us denote the number of nonzero rates to be exchanged by M and the number of information exchange bits to be used for quantization of each rate by n_f . BS m quantizes M rate terms, i.e., $r_m^{[c]}$, $c \in \mathcal{N}_G$, $m \in \mathcal{F}_c$. Thus, the number

Table 3: Achievable rates table for all the IFU selection cases for $N_T = 3$ and $N_C = 4$

	α	BS 1	BS 2	BS 3	BS 4
$\mathcal{F}_1 = \{1,2,3\}$	3	$r_1^{[1]}$	$r_2^{[1]}$	$r_3^{[1]}$	$r_4^{[1]}$
$\mathcal{F}_2 = \{1,2,4\}$	3	$r_1^{[2]}$	$r_2^{[2]}$	$r_3^{[2]}$	$r_4^{[2]}$
$\mathcal{F}_3 = \{1,3,4\}$	3	$r_1^{[3]}$	$r_2^{[3]}$	$r_3^{[3]}$	$r_4^{[3]}$
$\mathcal{F}_4 = \{2,3,4\}$	3	$r_1^{[4]}$	$r_2^{[4]}$	$r_3^{[4]}$	$r_4^{[4]}$
$\mathcal{F}_5 = \{1,2\}$	2	$r_1^{[5]}$	$r_2^{[5]}$	$r_3^{[5]}$	$r_4^{[5]}$
$\mathcal{F}_6 = \{1,3\}$	2	$r_1^{[6]}$	$r_2^{[6]}$	$r_3^{[6]}$	$r_4^{[6]}$
$\mathcal{F}_7 = \{1,4\}$	2	$r_1^{[7]}$	$r_2^{[7]}$	$r_3^{[7]}$	$r_4^{[7]}$
$\mathcal{F}_8 = \{2,3\}$	2	$r_1^{[8]}$	$r_2^{[8]}$	$r_3^{[8]}$	$r_4^{[8]}$
$\mathcal{F}_9 = \{2,4\}$	2	$r_1^{[9]}$	$r_2^{[9]}$	$r_3^{[9]}$	$r_4^{[9]}$
$\mathcal{F}_{10} = \{3,4\}$	2	$r_1^{[10]}$	$r_2^{[10]}$	$r_3^{[10]}$	$r_4^{[10]}$
$\mathcal{F}_{11} = \{1\}$	1	$r_1^{[11]}$	$r_2^{[11]}$	$r_3^{[11]}$	$r_4^{[11]}$
$\mathcal{F}_{12} = \{2\}$	1	$r_1^{[12]}$	$r_2^{[12]}$	$r_3^{[12]}$	$r_4^{[12]}$
$\mathcal{F}_{13} = \{3\}$	1	$r_1^{[13]}$	$r_2^{[13]}$	$r_3^{[13]}$	$r_4^{[13]}$
$\mathcal{F}_{14} = \{4\}$	1	$r_1^{[14]}$	$r_2^{[14]}$	$r_3^{[14]}$	$r_4^{[14]}$

$R_{\text{global}}^{[4]} \rightarrow$ not reported and replaced by $\bar{R}_{\text{global}}^{[4]}$

$R_{\text{local}}^{[4]}$: reported if $|\mathcal{F}_4| \in \mathcal{A}$.

If $\mathcal{A} = \{1,3\}$, each BS shares 4 $r_m^{[c]}$, $m \in \mathcal{F}_c$, $|\mathcal{F}_c| \in \mathcal{A}$.

$R_{\text{global}}^{[10]} \rightarrow$ not reported and replaced by $\bar{R}_{\text{global}}^{[10]}$

$R_{\text{local}}^{[10]}$: reported if $|\mathcal{F}_{10}| \in \mathcal{A}$.

$r_m^{[c]}$: can be attained with only local CSI at BS m , $m \in \mathcal{F}_c$

$r_n^{[c]}$: requires global CSI to be attained at BS n , $n \notin \mathcal{F}_c$

of information exchange bits used at each BS is

$$N_f = M \cdot n_f. \quad (81)$$

For optimal quantization, the probability density function (PDF) of $r_m^{[c]}$, $c = 1, \dots, N_K$, $m \in \mathcal{F}_c$, is needed, which is denoted by $f(t)$. To get the PDF $f(t)$, we establish the following lemma.

Lemma 5. *The random variable $|\mathbf{h}_{mm}^H \mathbf{w}_m^{[c]}|^2$, $c = 1, \dots, N_K$, $m \in \mathcal{F}_c$, is distributed as a Chi-square random variable with degrees of freedom (DoF) of $2(N_T - \alpha + 1)$.*

Proof. i) For $\alpha = N_T$, the beamforming vector $\mathbf{w}_m^{[c]}$ is designed to only minimize the GI to user n , $n \in \mathcal{F}_c \setminus \{m\}$. Thus, $\mathbf{w}_m^{[c]}$ is designed independently with the desired channel vector \mathbf{h}_{mm} and $|\mathbf{h}_{mm}^H \mathbf{w}_m^{[c]}|^2$ is distributed as a Chi-square random variable with DoF 2.

ii) For $\alpha \leq N_T - 1$, the beamforming vector $\mathbf{w}_m^{[c]}$ is designed to maximize its WSLNR and it has the direction of the orthogonal projection of \mathbf{h}_{mm} onto the null space of \mathbf{h}_{mn} , where $m \in \mathcal{F}_c$ and $n \in \mathcal{F}_c \setminus \{m\}$. Let us denote \mathbf{b}_p is the p -th basis vector of the null space of \mathbf{h}_{mn} . The number of the basis vector is $N_T - (\alpha - 1)$. Then, the desired channel gain can be represented as

$$|\mathbf{h}_{mm}^H \mathbf{w}_m^{[c]}|^2 = \left\| \sum_{p=1}^{N_T - \alpha + 1} |\mathbf{h}_{mm} \mathbf{b}_p| \cdot \mathbf{b}_p \right\|^2 = \sum_{p=1}^{N_T - \alpha + 1} |\mathbf{h}_{mm} \mathbf{b}_p|^2, \quad (82)$$

and it is the Chi-square random variable with DoF of $2(N_T - \alpha + 1)$. \square

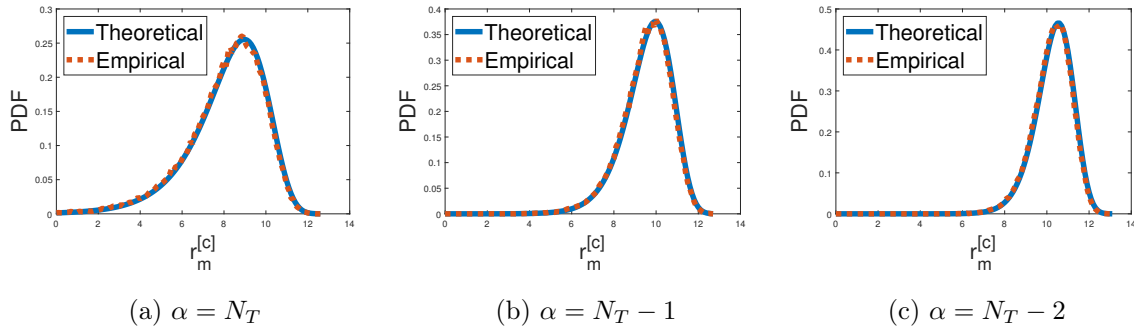


Figure 8: PDFs of $r_m^{[c]}$ for $N_T = 4$, and $N_C = 7$

In addition, using Lemma 5, the following theorem is established to derive $f(t)$ which is the PDF of $r_m^{[c]}$, $c = 1, \dots, N_K$, $m \in \mathcal{F}_c$.

Theorem 4. *The PDF of $r_m^{[c]}$, $c = 1, \dots, N_K$, $m \in \mathcal{F}_c$, is given by*

$$f(t) = \frac{2^t N_0^{N_T - \alpha + 1} \ln 2 (2^t - 1)^{N_T - \alpha}}{2^{N_T - \alpha + 1} \Gamma(N_T - \alpha + 1)} e^{-\frac{N_0(2^t - 1)}{2}}. \quad (83)$$

Proof. Let us denote the PDF of $\eta_{mm}^{[c]}$ as $h(t)$, the cumulative density function (CDF) of $\eta_{mm}^{[c]}$ as $H(t)$, and the CDF of $r_m^{[c]}$ as $F(t)$. From (80), we have $F(t) = H(N_0(2^t - 1))$ and

$$f(t) = \ln 2 \cdot N_0 \cdot 2^t \cdot h(N_0(2^t - 1)). \quad (84)$$

Since $h(t) = \frac{t^{N_T - \alpha} e^{-\frac{t}{2}}}{2^{N_T - \alpha + 1} \Gamma(N_T - \alpha + 1)}$ from the results of Lemma 5, $f(t)$ in (84) becomes (83), which proves the theorem. \square

The results in Fig. 8 show that the pdf of (83), denoted by ‘Theoretical,’ is well matched with the simulated histograms which are denoted by ‘Empirical’.

From the PDF of $r_m^{[c]}$ in Theorem 4, each $r_m^{[c]}$ is quantized with the Lloyd-max non-uniform quantization method minimizing the mean-square quantization error [48].

4.7 Information exchange protocol

There are two possible information exchange protocols. In the first possible protocol, referred to as ‘centralized protocol,’ one of the BSs calculates which users become the IFUs. A step-by-step illustration of the centralized protocol is depicted in Fig. 9. In the second possible protocol, referred to as ‘decentralized protocol,’ all the BSs share quantized M rates with the other BSs. Then, each BS determines the IFUs and designs the beamforming vector. The total amounts of information exchange bits of the centralized protocol and the decentralized protocol are denoted by $S_{\text{centralized}}$ and $S_{\text{decentralized}}$, respectively. Then, we have

$$S_{\text{central}} = (N_C - 1) \cdot N_f + (N_C - 1) \cdot \left[\log \left(\sum_{\alpha=1}^{N_T} \binom{N_C}{\alpha} \right) \right], \quad (85)$$

$$S_{\text{decentral}} = (N_C - 1) \cdot N_f + (N_C - 1) \cdot (N_C - 1) \cdot N_f. \quad (86)$$

Since $N_C \geq 3$ and $\sum_{\alpha=1}^{N_T} \binom{N_C}{\alpha} < N_T \sqrt{\frac{8}{\pi N_C}} \cdot 2^{N_C-1}$ from [56, Theorem 2.2], we have

$$\left\lceil \log \left(\sum_{\alpha=1}^{N_T} \binom{N_C}{\alpha} \right) \right\rceil \leq (N_C - 1) + \lceil \log N_T \rceil \quad (87)$$

$$< (N_C - 1) + N_T \quad (88)$$

$$\leq (N_C - 1) \cdot 2 \quad (89)$$

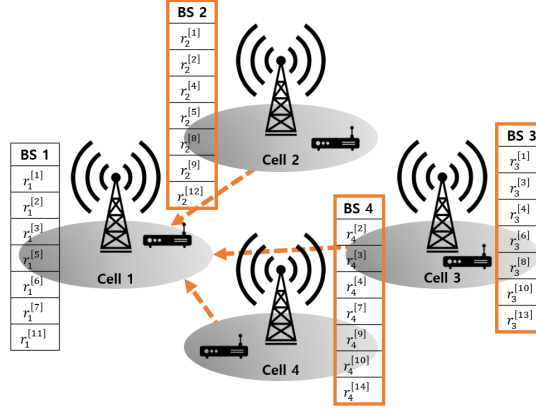
for $N_f \geq 2$. Thus, the centralized protocol is more preferable than the decentralized protocol, especially if $N_f \geq 2$, and hence we use the centralized protocol as shown in Fig. 9.

4.8 Information exchange comparison

In this subsection, the amount of information exchange required in the proposed scheme is compared to those of existing schemes. The distributed weighted minimizing mean-square error (WMMSE) scheme [44] is considered, where each beamforming vector is designed iteratively between the transmitters and receivers. It is known that the ‘WMMSE’ scheme is the most efficient scheme that iteratively achieves the optimal sum-rate bound but in a distributed manner. The number of iteration and the number of bits required for the quantization of each scalar or vector in the ‘WMMSE’ scheme are denoted by κ and n_f^{WMMSE} , respectively. The ‘Global’ scheme is also considered, where all the beamforming vectors are jointly optimized in pursuit of maximizing the sum-rate with global CSI [5]. Let us denote the number of bits required for the quantization of each vector in the ‘Global’ scheme by n_f^{Global} . Then, Table 4 summarizes the amount of required information exchange in bytes for the considered schemes. As shown in Table 4, the amount of the required information exchange of the propose scheme is much less than those of ‘WMMSE’ and ‘Global’. Moreover, the required information exchange of ‘WMMSE’ increases in proportion to the number of iteration κ . Unlike ‘WMMSE’ and ‘Global,’ the information required to be exchanged among BSs for the proposed scheme is merely scalar values. Therefore, the amount of information exchange does not increase even for growing N_T , which significantly lowers the burden of the backhaul or direct link.

4.9 Extension to the Multiuser Case

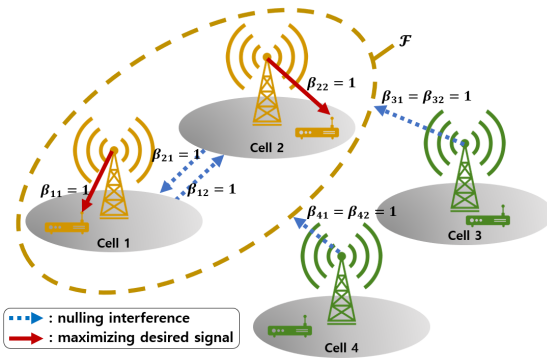
In this section, the proposed scheme is extended to the multiuser case, where each cell is composed of N_U users. The p -th user in the i -th cell is referred to as user i_p , where $i \in \mathcal{N}_C$, $p \in \{1, \dots, N_U\} \triangleq \mathcal{N}_U$, and $i_p \in \{i_p | i \in \mathcal{N}_C, p \in \mathcal{N}_U\} \triangleq \mathcal{N}_W$. It is assumed that $N_T < N_U N_C$. The channel vector from BS i to user j_r is denoted by \mathbf{h}_{i,j_r} . The received signal at user i_p is



(a)

	α	BS 1	BS 2	BS 3	BS 4
$\mathcal{F}_1 = \{1,2,3\}$	3	$r_1^{[1]}$	$r_2^{[1]}$	$r_3^{[1]}$	$r_4^{[1]}$
$\mathcal{F}_2 = \{1,2,4\}$	3	$r_1^{[2]}$	$r_2^{[2]}$	$r_3^{[2]}$	$r_4^{[2]}$
$\mathcal{F}_3 = \{1,3,4\}$	3	$r_1^{[3]}$	$r_2^{[3]}$	$r_3^{[3]}$	$r_4^{[3]}$
$\mathcal{F}_4 = \{2,3,4\}$	3	$r_1^{[4]}$	$r_2^{[4]}$	$r_3^{[4]}$	$r_4^{[4]}$
$\mathcal{F}_5 = \{1,2\}$	2	$r_1^{[5]}$	$r_2^{[5]}$	$r_3^{[5]}$	$r_4^{[5]}$
$\mathcal{F}_6 = \{1,3\}$	2	$r_1^{[6]}$	$r_2^{[6]}$	$r_3^{[6]}$	$r_4^{[6]}$
$\mathcal{F}_7 = \{1,4\}$	2	$r_1^{[7]}$	$r_2^{[7]}$	$r_3^{[7]}$	$r_4^{[7]}$
$\mathcal{F}_8 = \{2,3\}$	2	$r_1^{[8]}$	$r_2^{[8]}$	$r_3^{[8]}$	$r_4^{[8]}$
$\mathcal{F}_9 = \{2,4\}$	2	$r_1^{[9]}$	$r_2^{[9]}$	$r_3^{[9]}$	$r_4^{[9]}$
$\mathcal{F}_{10} = \{3,4\}$	2	$r_1^{[10]}$	$r_2^{[10]}$	$r_3^{[10]}$	$r_4^{[10]}$
$\mathcal{F}_{11} = \{1\}$	1	$r_1^{[11]}$	$r_2^{[11]}$	$r_3^{[11]}$	$r_4^{[11]}$
$\mathcal{F}_{12} = \{2\}$	1	$r_1^{[12]}$	$r_2^{[12]}$	$r_3^{[12]}$	$r_4^{[12]}$
$\mathcal{F}_{13} = \{3\}$	1	$r_1^{[13]}$	$r_2^{[13]}$	$r_3^{[13]}$	$r_4^{[13]}$
$\mathcal{F}_{14} = \{4\}$	1	$r_1^{[14]}$	$r_2^{[14]}$	$r_3^{[14]}$	$r_4^{[14]}$

(b)



(c)

Figure 9: Example of the overall beamforming vectors design and information exchange protocol for $N_T = 3$, $N_C = 4$, and $\mathcal{A} = \{1, 2, 3\}$: (a) BS m calculates the rates $r_m^{[c]}$ in (80), $c \in \mathcal{N}_G$, $m \in \mathcal{F}_c$, which can be calculated with only local CSI and shares them with BS 1 through the information exchange. (b) BS 1 gathers all the $r_m^{[c]}$ and makes an table on the left side of Fig. 9b. The white cells in the table are the shared rates by other BSs. Then, BS 1 chooses the set of the IFUs as (79). The index of the set of the IFUs is noticed through the information exchange. (c) All the BSs design beamforming vectors which make zero interference to the users with the index which is selected in Fig. 9b. In this example, selected α is $2 = N_T - 1$ and selected $\mathcal{F} = \{1, 2\}$, and hence all the BSs design beamforming vectors as Fig. 7b.

Table 4: Amount of required information exchange

Scheme	Amount of information exchange (bytes)		
	General expression (bits)	$N_T = 4, N_C = 7,$ $N_f = 35, \kappa = 2,$ $n_f^{\text{WMMSE}} = n_f^{\text{Global}} = 2$	$N_T = 8, N_C = 9,$ $N_f = 84, \kappa = 2,$ $n_f^{\text{WMMSE}} = n_f^{\text{Global}} = 5$
Proposed	$(N_C - 1) \cdot \left(N_f + \left\lceil \log(\sum_{\alpha=1}^{N_T} \binom{N_C}{\alpha}) \right\rceil \right)$	32	91
WMMSE	$3\kappa n_f^{\text{WMMSE}} N_C^2$	74	304
Global	$n_f^{\text{Global}} N_C^2 (N_C - 1)$	74	405

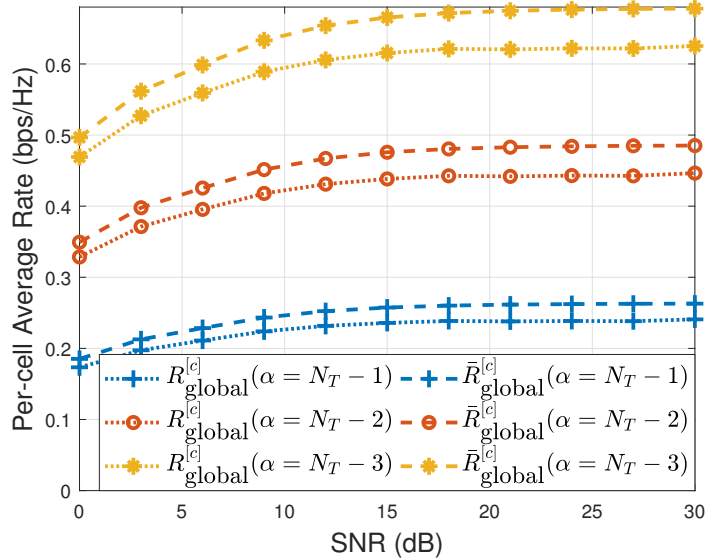


Figure 10: Per-cell average $R_{\text{global}}^{[c]}$ and $\bar{R}_{\text{global}}^{[c]}$ versus SNR for $N_T = 4$ and $N_C = 7$

written by

$$y_{i_p} = \underbrace{\mathbf{h}_{i,i_p} \mathbf{w}_{i_p} x_{i_p}}_{\text{desired signal}} + \underbrace{\sum_{q \in \mathcal{N}_C \setminus \{p\}} \mathbf{h}_{i,i_p} \mathbf{w}_{i_q} x_{i_q}}_{\text{intracell interference}} + \underbrace{\sum_{j \in \mathcal{N}_C \setminus \{i\}} \sum_{r \in \mathcal{N}_U} \mathbf{h}_{j,i_p} \mathbf{w}_{j_r} x_{j_r}}_{\text{intercell interference}} + z_{i_p}, \quad (90)$$

where x_{l_k} is the unit-variance transmit symbol at BS l to user l_k and z_{l_k} is the AWGN at user l_k with zero-mean and variance of N_0 . Thus, the corresponding SINR is expressed by

$$\gamma_{i_p} = \frac{|\mathbf{h}_{i,i_p} \mathbf{w}_{i_p}|^2}{\sum_{q \in \mathcal{N}_U \setminus \{p\}} |\mathbf{h}_{i,i_p} \mathbf{w}_{i_q}|^2 + \sum_{j \in \mathcal{N}_C \setminus \{i\}} \sum_{r \in \mathcal{N}_U} |\mathbf{h}_{j,i_p} \mathbf{w}_{j_r}|^2 + N_0}, \quad (91)$$

and the achievable sum-rate is given by

$$R_M = \sum_{i \in \mathcal{N}_C} \sum_{p \in \mathcal{N}_U} \log(1 + \gamma_{i_p}). \quad (92)$$

As shown in (48), the sum-rate maximization problem can be obtained by solving the max-WSLNR problem. Let us denote the weight coefficient for the channel gain from BS i to user j_r by $\beta_{i,j_r} \geq 0$ and the set of β_{i,j_r} , $j_r \in \mathcal{N}_W$, by $\boldsymbol{\beta}_i = \{\beta_{i,j_r} | j_r \in \mathcal{N}_W\}$. As the single user case, β_{i,j_r} is restricted to $\beta_{i,j_r} \in \{0, 1\}$ and then a general WSLNR incorporating the notion of WGI is defined as follows:

$$\chi_{i_p} = \begin{cases} \beta_{i,i_p} |\mathbf{h}_{i,i_p} \mathbf{w}_{i_p}|^2 / (P_{i_p} + N_0) & \text{if } \beta_{i,i_p} \neq 0 \\ 1 / (P_{i_p} + N_0) & \text{if } \beta_{i,i_p} = 0, \end{cases} \quad (93)$$

where

$$P_{i_p} = \sum_{q \in \mathcal{N}_U \setminus \{p\}} \beta_{i,i_q} |\mathbf{h}_{i,i_q} \mathbf{w}_{i_p}|^2 + \sum_{j \in \mathcal{N}_C \setminus \{i\}} \sum_{r \in \mathcal{N}_U} \beta_{i,j_r} |\mathbf{h}_{i,j_r} \mathbf{w}_{i_p}|^2. \quad (94)$$

In this section, the set of all the IFUs is denoted by $\mathcal{F}_M \subset \mathcal{N}_W$, and the number of IFUs as α_M .

4.9.1 Beamforming vector design for $|\mathcal{F}_M| = N_T$

Suppose that user m_p is an IFU. Then, the interference-free constraints at the receiver side are given by

$$\mathbf{h}_{k,m_p}^H \mathbf{w}_{k_l} = 0, \quad k_l \in \mathcal{N}_W \setminus \{m_p\}. \quad (95)$$

The number of these equalities for the α_M IFUs is $\alpha_M((N_U - 1) + (N_A - 1)N_U)$ assuming N_A is the number of BSs with non-zero transmission power. On the other hand, the number of effective variables in each \mathbf{w}_{k_l} is $N_T - 1$ considering the unit-norm constraint. For the existence of the solution on \mathbf{w}_{k_l} of the equalities (95), we need the number of effective variables to be equal to or greater than the number of equalities, i.e., $\alpha_M((N_U - 1) + (N_A - 1)N_U) \leq N_A N_U (N_T - 1) \iff \alpha_M \leq \frac{N_A N_U (N_T - 1)}{N_A N_U - 1}$. Therefore, the maximum number of IFUs in the MISO interference channel for multiuser case is given by

$$\alpha_{M,\max} = \begin{cases} N_T & \text{if } N_A = N_T / N_U \\ N_T - 1 & \text{if } N_A > N_T / N_U \\ N_A N_U & \text{otherwise.} \end{cases} \quad (96)$$

As shown in (96), $|\mathcal{F}_M| = N_T$ can be achieved only when N_T is divisible by N_U . If $\frac{N_T}{N_U}$ is a natural number, there exist $\left(\frac{N_C}{\frac{N_T}{N_U}}\right)$ possible IFUs selection for $|\mathcal{F}_M| = N_T$.

The N_T IFUs can be obtained by muting $(N_C - \frac{N_T}{N_U})$ BSs. In such a case, all the users in the cells where the BSs have non-zero transmission power are the IFUs. BS m which has non-zero transmission power designs beamforming vectors that maximize (93) setting $\beta_{m,m_p} = 0$, $\beta_{m,k_l} = 1$ for $k_l \in \mathcal{F}_M \setminus \{m_p\}$, and $\beta_{m,n_r} = 1$ for $n_r \in \mathcal{N}_W \setminus \mathcal{F}_M$ as

$$\mathbf{w}_{m_p}^{\text{min-WGI}} = \arg \max_{\|\mathbf{w}\|^2=1} \frac{1}{\sum_{k_l \in \mathcal{F}_M \setminus \{m_p\}} |\mathbf{h}_{m,k_l}^H \mathbf{w}|^2 + N_0} \quad (97)$$

$$= \arg \min_{\|\mathbf{w}\|^2=1} \|\mathbf{G}_{m_p} \mathbf{w}\|^2, \quad (98)$$

where $\mathbf{G}_{m_p} \triangleq \left[\sqrt{\beta_{m,1_1}} \mathbf{h}_{m,1_1}, \dots, \sqrt{\beta_{m,N_C N_U}} \mathbf{h}_{m,N_C N_U} \right]^H \in \mathbb{C}^{N_C N_U \times N_T}$. Then, the solution of (97) is obtained by choosing the right singular vector of \mathbf{G}_{m_p} associated with the smallest singular value.

4.9.2 Beamforming vector design for $|\mathcal{F}_M| = N_T - 1$

For $|\mathcal{F}_M| = N_T - 1$, all the BSs have non-zero transmission power.

4.9.2.1 Design of \mathbf{w}_{n_r} for $n_r \in \mathcal{N}_W \setminus \mathcal{F}_M$: BS n designs beamforming vector \mathbf{w}_{n_r} , $n_r \in \mathcal{N}_W \setminus \mathcal{F}_M$, to make user m_p , $m_p \in \mathcal{F}_M$, interference-free. Thus, the beamforming vector design of \mathbf{w}_{n_r} for $n_r \in \mathcal{N}_W \setminus \mathcal{F}_M$ employ the min-WGI beamforming design in (97).

4.9.2.2 Design of \mathbf{w}_{m_p} for $m_p \in \mathcal{F}$: Since BS m designs the beamforming vector \mathbf{w}_{m_p} , $m_p \in \mathcal{F}$, only making zero interference to the users with the indices in $\mathcal{F} \setminus \{m_p\}$, where $|\mathcal{F} \setminus \{m_p\}| = N_T - 2$, BS m utilizes the space of rank one to improve the channel gain. Then, \mathbf{w}_{m_p} is designed maximizing (93) with $\beta_{m,m_p} = \beta_{m,k_l} = 1$ for $k_l \in \mathcal{F} \setminus \{m_p\}$ and $\beta_{m,n_r} = 0$ for $n_r \in \mathcal{N}_W \setminus \mathcal{F}$.

4.9.3 Beamforming vector design for $|\mathcal{F}_M| \leq N_T - 2$

For $|\mathcal{F}_M| = \alpha_M \leq N_T - 2$, all the BSs designs the beamforming vectors making zero interference to user m_p , $m_p \in \mathcal{F}_M$. The number of neighboring users, to which each BS makes GI zero, is $\alpha_M - 1$ for the beamforming vector design of \mathbf{w}_{m_p} , $m_p \in \mathcal{F}_M$, and α_M for the beamforming vector design of \mathbf{w}_{n_r} , $n_r \in \mathcal{N}_W \setminus \mathcal{F}_M$. Then, the beamforming vectors \mathbf{w}_{m_p} and \mathbf{w}_{n_r} are designed in the null space of ranks $(N_T - \alpha_M + 1)$ and $(N_T - \alpha_M)$, respectively. Thus, BS m designs the beamforming vectors \mathbf{w}_{m_p} maximizing (93) by setting $\beta_{m,m_p} = \beta_{m,k_l} = 1$, $m_p \in \mathcal{F}_M$, $k_l \in \mathcal{F}_M \setminus \{m_p\}$, and $\beta_{m,n_r} = 0$, $n_r \in \mathcal{N}_W \setminus \mathcal{F}_M$. BS n designs the beamforming vectors \mathbf{w}_{n_r} maximizing (93) by setting $\beta_{n,m_p} = \beta_{n,n_r} = 1$, $m_p \in \mathcal{F}_M$, $n_r \in \mathcal{N}_W \setminus \mathcal{F}_M$, and $\beta_{n,v_g} = 0$, $v_g \in \mathcal{N}_W \setminus (\mathcal{F}_M \cup \{n_r\})$.

Since BS m designs the beamforming vector \mathbf{w}_{m_p} , $m_p \in \mathcal{F}_M$, only making zero interference to the users with the indices in $\mathcal{F}_M \setminus \{m_p\}$, where $|\mathcal{F}_M \setminus \{m_p\}| = \alpha_M - 1$, BS m utilizes the space of rank $(N_T - \alpha_M + 1)$ to improve the channel gain. Then, \mathbf{w}_{m_p} is designed maximizing (93) with $\beta_{m,m_p} = \beta_{m,k_l} = 1$ for $k_l \in \mathcal{F}_M \setminus \{m_p\}$ and $\beta_{m,n_r} = 0$ for $n_r \in \mathcal{N}_W \setminus \mathcal{F}_M$.

4.9.4 Selection of \mathcal{F}_M : Design of β_{i,k_l}

There exist $\binom{N_C}{N_T} + \binom{N_C N_U}{N_T - 1} + \dots + \binom{N_C N_U}{1}$ possible IFUs selection if N_T is divisible by N_U and $\binom{N_C N_U}{N_T - 1} + \dots + \binom{N_C N_U}{1}$ possible IFUs selection otherwise. Let us denote the c -th IFU selection as $\mathcal{F}_c^{[M]}$. Then, the sum-rate for the c -th IFUs selection can be represented as

$$R_M^{[c]} = R_{\text{local},M}^{[c]} + R_{\text{global},M}^{[c]}, \quad (99)$$

where $R_{\text{local},M}^{[c]} = \sum_{m_p \in \mathcal{F}_c^{[M]}} \log \left(1 + \frac{\eta_{m_p, m_p}^{[c]}}{N_0} \right)$, $R_{\text{global},M}^{[c]} = \sum_{n_r \in \mathcal{N}_W \setminus \mathcal{F}_c^{[M]}} \log \left(1 + \frac{\eta_{n_r, n_r}^{[c]}}{T_{n_r}^{[c]}} \right)$, $\eta_{i_p, j_q}^{[c]} = |\mathbf{h}_{j, i_p} \mathbf{w}_{j_q}^{[c]}|^2$, and $T_{n_r}^{[c]} = \sum_{s \in \mathcal{N}_U \setminus \{r\}} \eta_{n_r, n_s}^{[c]} + \sum_{k \in \mathcal{N}_C \setminus \{n\}} \sum_{l \in \mathcal{N}_U} \eta_{n_r, k_l}^{[c]} + N_0$.

We propose to select the index set \mathcal{F} which maximizes $R_{\text{local},M}^{[c]} + \bar{R}_{\text{global},M}^{[c]}$, where

$$\bar{R}_{\text{global},M}^{[c]} = (N_C N_U - \alpha_M) \log \left(1 + \frac{(N_T - \alpha_M) \Gamma \left(2 - N_C N_U, \frac{N_0}{2} \right)}{e^{-\frac{N_0}{2}} \left(\frac{N_0}{2} \right)^{2 - N_C N_U}} \right) \quad (100)$$

is the upper bound of $E\{R_{\text{global},M}^{[c]}\}$, which can be obtained from Lemma 4 by considering both intercell interference and intracell interference. At this point, let us assume that the information is collected only for the cases with selected α_M as in Section 4.4. In case, let us denote the set of considered α_M and the index set of the considered cases as \mathcal{A}_M and \mathcal{N}_G^M , respectively. For example, if the set of considered α_M is $\mathcal{A}_M = \{N_T - 1, N_T\}$ for $N_T = 3$, $N_C = 4$, and $N_U = 3$, we have $|\mathcal{N}_G^M| = \binom{N_C}{N_T} + \binom{N_C N_U}{N_T - 1} = 70$.

Finally, the index set \mathcal{F}_M can be found from

$$\mathcal{F}_M = \mathcal{F}_{c^*}^{[M]} \quad (101)$$

$$c^* = \arg \max_{c \in \mathcal{N}_G} R_{\text{local},M}^{[c]} + \bar{R}_{\text{global},M}^{[c]}. \quad (102)$$

4.10 Numerical Simulations

Figures 11 and 12 demonstrate the average achievable rate per-cell versus SNR for $(N_T = 4, N_C = 7)$ and $(N_T = 8, N_C = 9)$, respectively, under Rayleigh fading environment. In Figs. 11a and 12a, the existing schemes discussed in Section 4.8 are compared with the proposed scheme. For ‘WMMSE’ and ‘Global,’ the set of $(\kappa, n_f^{\text{WMMSE}}, n_f^{\text{Global}})$ is assumed to be $(2, 2, 2)$ for $(N_T = 4, N_C = 7)$ and $(2, 5, 5)$ for $(N_T = 8, N_C = 9)$, respectively, for fair comparison of the amount of the information exchange. In addition, three schemes requiring only local CSI without information exchange are also considered as follows. First, ‘Max-SNR’ is considered, in which all

the beamforming vectors are designed only to maximize the channel gain of the desired channels. Second, ‘Min-GI’ [7] is considered, where all the beamforming vectors are determined only to minimize GI. Third, in ‘Max-SLNR’ [4], all the beamforming vectors are constructed maximizing SLNR. In the baseline ‘Random’ scheme, each beamforming vector is randomly determined. To show the impact of the process of determination of α and \mathcal{F} , ‘Proposed-unquantized-random1’ and ‘Proposed-unquantized-random2’ are considered. In ‘Proposed-unquantized-random1,’ α is selected by the proposed algorithm and \mathcal{F} is randomly selected for given α . In ‘Proposed-unquantized-random2,’ both α and \mathcal{F} are randomly chosen. For the comparison, unquantized versions of ‘WMMSE,’ ‘Global,’ and the proposed scheme are considered.

In Fig. 11a, ‘Max-SLNR’ shows the highest performance among the schemes which require local CSI only. In case of ‘Proposed-unquantized,’ it shows the per-cell average rate close to the optimal performance, i.e., ‘Global-unquantized,’ in the SNR regime higher than 15dB. In the figure, ‘Proposed ($\mathcal{A} = \{N_T - 1, N_T\}$, $N_f = 35$)’ shows 6~11% performance improvement compared to that of ‘Proposed-unquantized-random1’; that is, the proposed scheme has notable advantage in performance only with 35 bits of information exchange per-cell by selecting a proper set of IFUs, \mathcal{F} . On the other hand, ‘Proposed-unquantized-random1’ shows 17~32% per-cell average rate improvement compared with that of ‘Proposed-unquantized-random2,’ confirming the advantage of selecting a proper number of IFUs, α . In Fig. 12a, the performances of ‘Min-GI’ and ‘Max-SLNR’ are higher than those with $N_T = 4$, since the number of antennas is increased, resulting in lowered GI in cases of ‘Min-GI’ and ‘Max-SLNR’. With the increased number of antennas, the performance of the proposed scheme is closer to that of ‘Global-unquantized’ than the case of $N_T = 4$ in Fig. 11a. Because of the increased number of cells and antennas, N_K is also increased; that is, the number of bits required for the information exchange is increased. However, in Fig. 12a, the proposed scheme with reasonable amount of information exchange, ‘Proposed ($\mathcal{A} = \{N_T - 2, N_T - 1\}$, $N_f = 84$)’, still shows 4~8% improvement compared to that of ‘Proposed-unquantized-random1’.

In Figs. 11b and 12b, the impact of α is investigated by evaluating the performance of the proposed scheme but with fixed α . As seen from the figure, the best α value which means the α value with which the proposed scheme shows the maximum per-cell average rate increases from $N_T - 2$ to N_T for $N_T = 4$ and from $N_T - 3$ to $N_T - 1$ for $N_T = 8$, respectively, as SNR increases; that is, the same intuition from Fig. 6 is confirmed with the proposed scheme.

Table 5 summarizes the amount of the required computational complexity in order of flops for the proposed scheme, ‘WMMSE,’ and ‘Global-unquantized’. In ‘Global-unquantized’, the interior point method is used with iterations, where the number of maximum iterations is denoted as I_{\max} . As shown in Table 5 and Figs. 11a and 12a, the ‘Global-unquantized’ scheme requires excessive computational complexity compared to the other schemes to optimize all the beamforming vectors jointly. In particular, the computational complexity of the ‘WMMSE’ and ‘Global-unquantized’ schemes increases as the number of iterations, κ and I_{\max} , respectively. The computational complexity of the proposed scheme is much lower than that of ‘WMMSE’,

Table 5: Amount of required computational complexity in order of flops

scheme	Computational complexity in order of flops for $\kappa = 2$ and $I_{\max} = 10^2$		
	General expression	$N_T = 4, N_C = 7, M = 35$	$N_T = 8, N_C = 9, M = 84$
Proposed	$\mathcal{O}(N_T N_C (M + N_T^2))$	$1.43 \cdot 10^3$	$1.07 \cdot 10^4$
WMMSE	$\mathcal{O}(\kappa N_T^2 N_C (N_T + N_C))$	$2.46 \cdot 10^3$	$1.96 \cdot 10^4$
Global-unquantized	$\mathcal{O}(I_{\max} N_C^3 (N_T + 2)^3)$	$7.41 \cdot 10^6$	$7.29 \cdot 10^7$

while the per-cell average rate of the proposed scheme is much higher than that of ‘WMMSE’.

In Fig. 13, the per-cell average rates of the proposed scheme versus SNR are depicted for $(N_T = 4, N_C = 7, N_f = 42)$. For fixed N_f , four different sets of (n_f, M) are evaluated for $(N_T = 4, N_C = 7)$. In the SNR regime lower than 10dB, the proposed scheme with $\mathcal{A} = \{N_T - 2, N_T - 1\}$, $n_f = 2$, and $M = 21$ shows the maximum per-cell average rate compared to the other sets of (n_f, M) for fixed N_f . In the SNR regime higher than 10dB, the proposed scheme with $\mathcal{A} = \{N_T - 3, N_T\}$, $n_f = 2$, and $M = 21$ shows the maximum per-cell average rate compared with the other sets of (n_f, M) for fixed N_f . As shown in this figure, the proper selection of \mathcal{A} is crucial to maximize the per-cell average rate.

In Fig. 14, the relative per-cell average rates of the proposed scheme and ‘Max-SLNR’ normalized to the per-cell average rate of ‘Global-unquantized’ for SNR of -5~25dB are depicted for $(N_T = 8, N_C = 9, 10, 11, 12)$. As shown in Fig. 14, ‘Proposed-unquantized’ achieves 97% of the per-cell average rate of ‘Global-unquantized’, showing higher performance than the proposed schemes with fixed α . This implies that the proposed scheme adapts α well for changing system parameters, e.g., N_C and SNR, almost achieving the optimal performance requiring global CSI and joint beamforming vectors optimization. It is worthwhile to note that the proposed scheme shows much higher per-cell average rate gain compared to ‘Max-SLNR’ by finding proper weight coefficients for the SLNR equations.

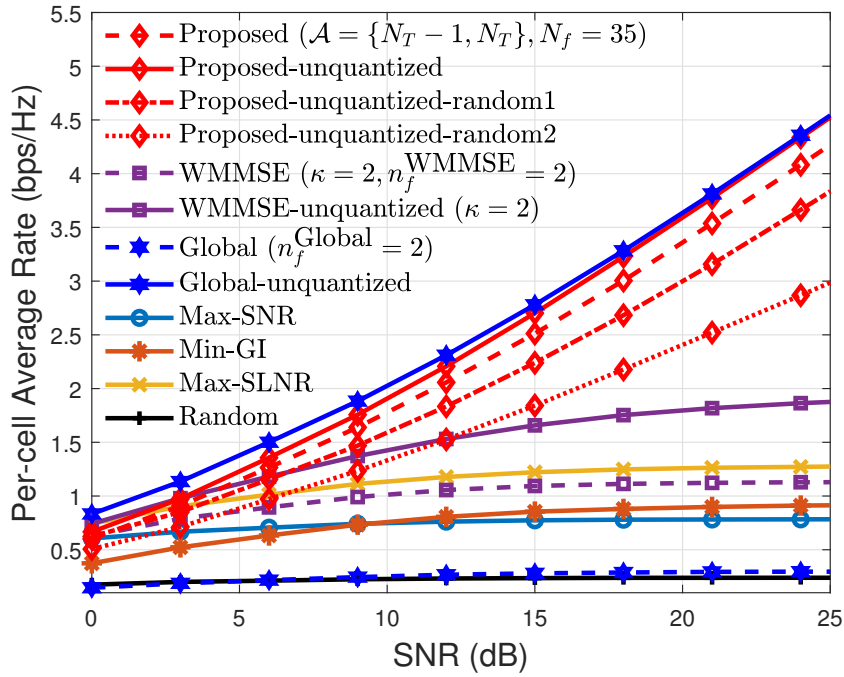
Figure 15 shows the probability that each α value is chosen in the proposed scheme for $(N_T = 8, N_C = 9, 10, 11, 12)$. As shown in these figures, the proposed scheme well adapts α values for varying environment, showing its robustness to changes of the system parameters.

In Figs. 16a and 16b, the relative per-cell average rates normalized to the per-cell average rate of ‘Global-unquantized’ vs. the amount of required information exchange of the proposed scheme are demonstrated compared to those of ‘WMMSE’ and ‘Global’ in the cases of $(N_T = 4, N_C = 7)$ and $(N_T = 8, N_C = 9)$, respectively. Note that for a variety of α values the amount of information exchange and the per-cell average rate gain vary, obtaining a flexible trade-off between the amount of information exchange and the per-cell average rate. In the case of $(N_T = 4, N_C = 7)$, the per-cell average rates of the proposed schemes with $\mathcal{A} = \{N_T - 1\}$ and $\mathcal{A} = \{N_T\}$ achieve 40% and 42% higher normalized per-cell average rate, respectively, compared to ‘WMMSE’ even with smaller amount of information exchange. When $\mathcal{A} = \{N_T - 1, N_T\}$

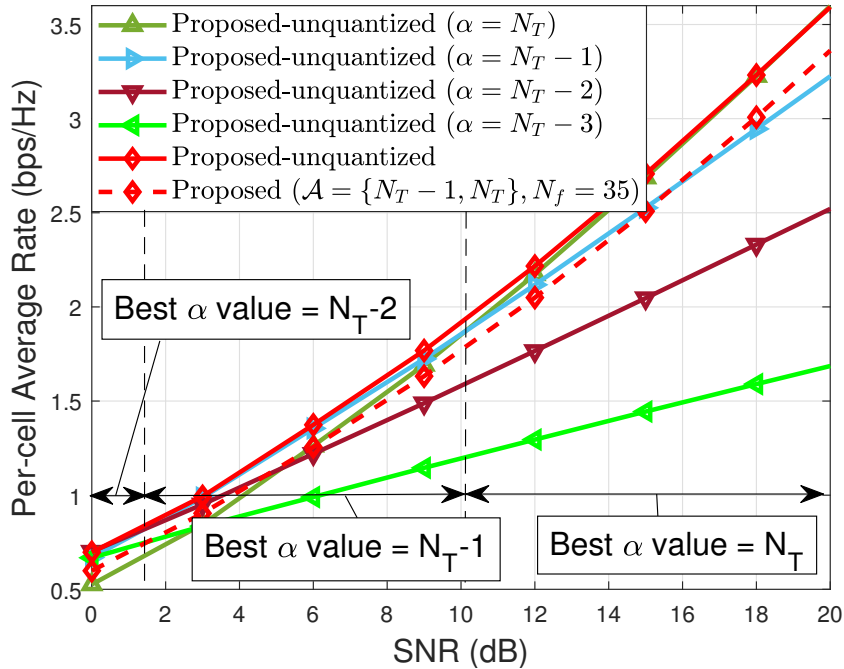
is considered, the proposed scheme achieves 45% higher normalized per-cell average rate than that of ‘WMMSE’. In the cases of ‘Global’ with $n_f^{\text{Global}} = 2$ and $n_f^{\text{Global}} = 18$, the normalized per-cell average rates of ‘Global’ are much lower than that of the proposed scheme while the required information exchange of ‘Global’ is much higher than that of the proposed scheme since much more bits are required for the exchange of quantized channel vector information in ‘Global’ compared to the scalar quantization of the proposed scheme. In the case of $(N_T = 8, N_C = 9)$, the proposed scheme with $\mathcal{A} = \{N_T - 2, N_T - 1\}$ exhibits 50% higher rate gain than ‘WMMSE’ with much smaller amount of information exchange. Compared to the case of $(N_T = 4, N_C = 7)$ in Fig. 12a, the required information exchange for the quantization of ‘Global’ increases due to increased N_T and N_C . As a result, the rate gain of ‘Global’ decreases due to the increased dimension of each channel vector to be quantized. As shown in Figs. 16a and 16b, there exists a trade-off in the proposed scheme between the rate gain and the amount of information exchange. However, when compared to the other existing schemes, the proposed scheme exhibits superior performance both in the sum-rate and the amount of information exchange due to the well structured beamforming design and information exchange protocol.

Figures 17a and 18a demonstrate the per-cell average rate versus transmission power for the single user small cell network with $(N_T = 4, N_C = 7)$ and the multiuser small cell network with $(N_T = 4, N_C = 7, N_U = 2)$, respectively. Figures 17b and 18b shows the cell configurations in small cell networks [57] for 17a and 18a, respectively. Assuming separate frequency carrier for the macro-cell BSs, e.g., Scenario 2a of the 3GPP small cell scenarios [18], there is no interference from the macro-cell BSs. Parameters and node droppings were selected from the 3GPP standards [18, 57] and simulation methodology therein.

As shown in Fig. 17a, the per-cell average rates of the considered schemes except the proposed scheme and ‘Global-unquantized’ are almost constant while that of the proposed scheme increases as the transmission power increases by mitigating intercell interference effectively. ‘Proposed-unquantized’ and the proposed scheme with only $N_f = 35$, i.e., 35 bits of information exchange per cell, achieve about 96% and 90% of ‘Global-unquantized,’ respectively, for the transmission power of 24~30dB. In Fig. 18a, the zero-forcing multiuser beamforming with local CSI, labeled as ‘ZF’, and the capacity-achieving dirty-paper coding precoding with local CSI [58], labeled as ‘DPC’, are additionally evaluated for comparison. It is shown that the proposed scheme with 17 bytes, i.e., 135 bits, of information exchange per cell achieves around 94% of ‘Proposed-unquantized,’ while ‘Proposed-unquantized’ achieves around 89% of ‘Global-unquantized’.

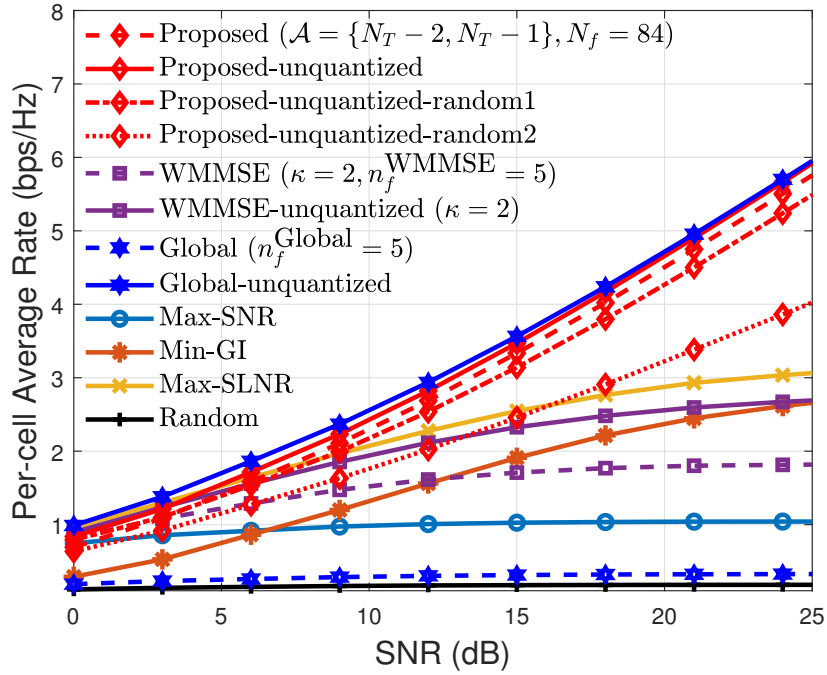


(a) Per-cell average rate versus SNR of the proposed scheme compared to the existing schemes

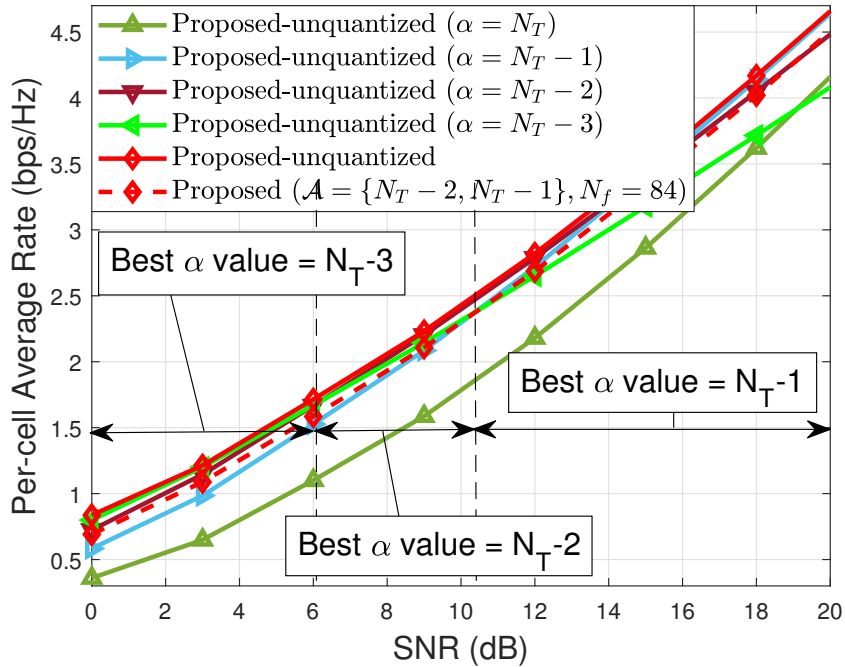


(b) Per-cell average rate versus SNR of the proposed scheme compared to the unquantized versions of the proposed scheme

Figure 11: Per-cell average rate versus SNR for $N_T = 4$ and $N_C = 7$



(a) Per-cell average rate versus SNR of the proposed scheme compared to the existing schemes



(b) Per-cell average rate versus SNR of the proposed scheme compared to the unquantized versions of the proposed scheme

Figure 12: Per-cell average rate versus SNR for $N_T = 8$ and $N_C = 9$

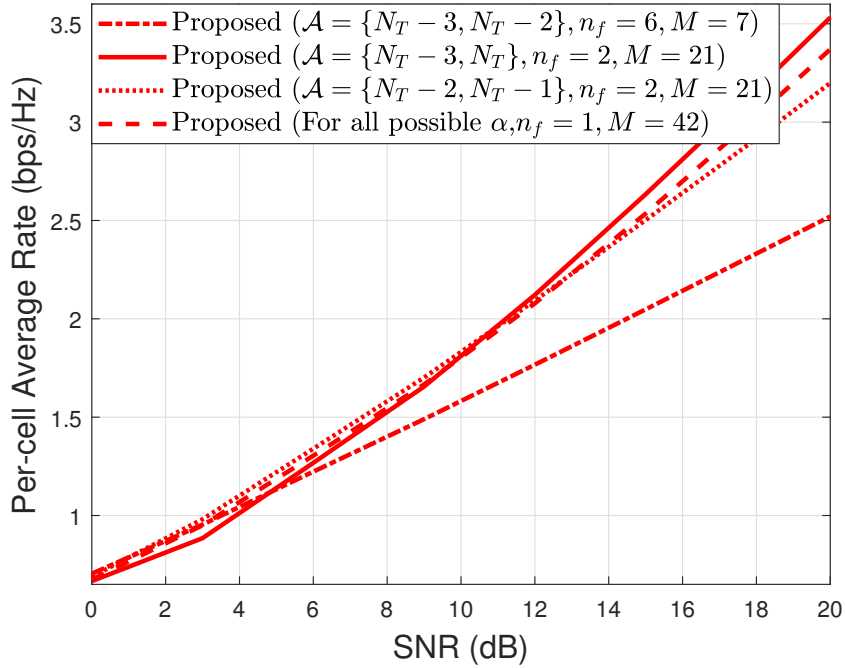


Figure 13: Per-cell average rate versus SNR of the proposed scheme for $N_T = 4$, $N_C = 7$, and $N_f = 42$

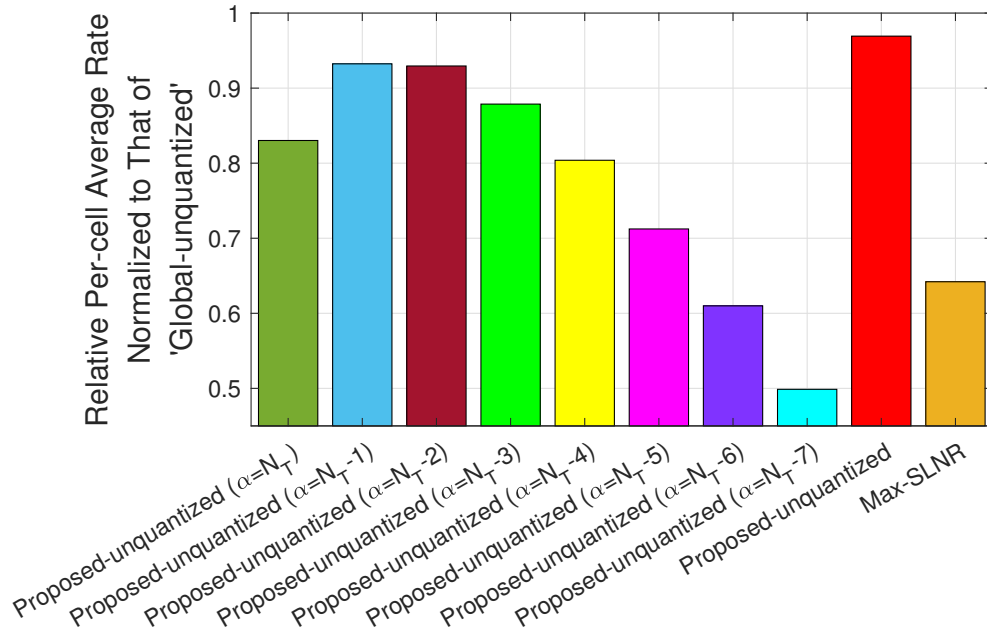


Figure 14: Per-cell average rate versus SNR of the proposed scheme for $N_T = 8$, $N_C = 9$, and $N_f = 250$

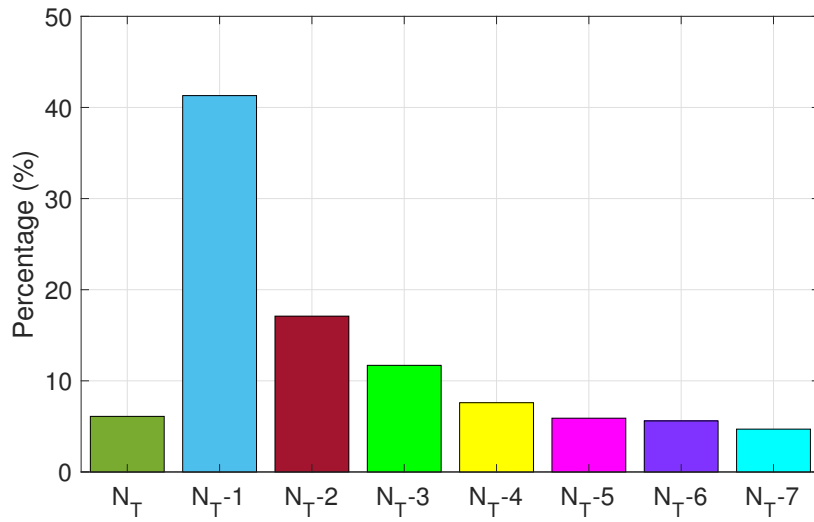
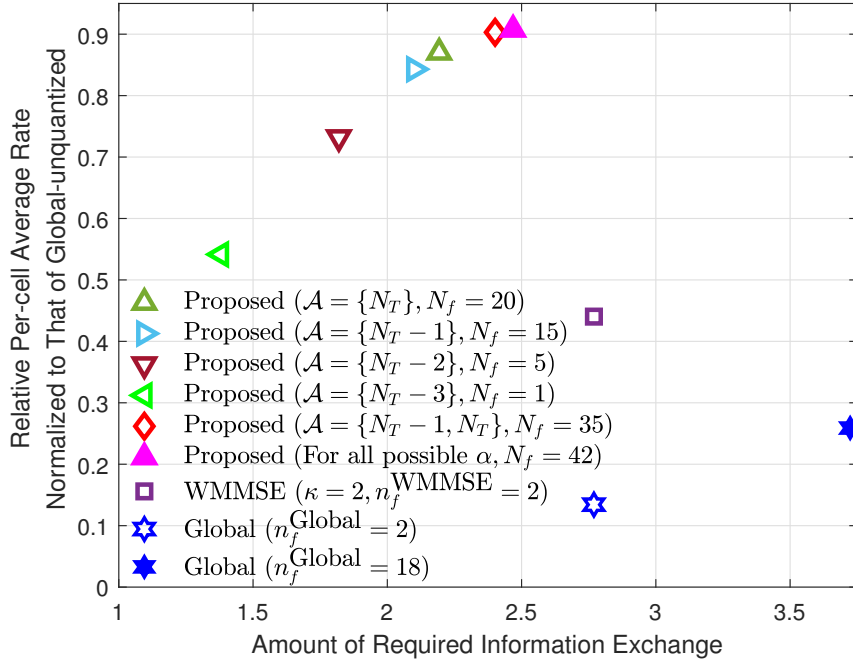
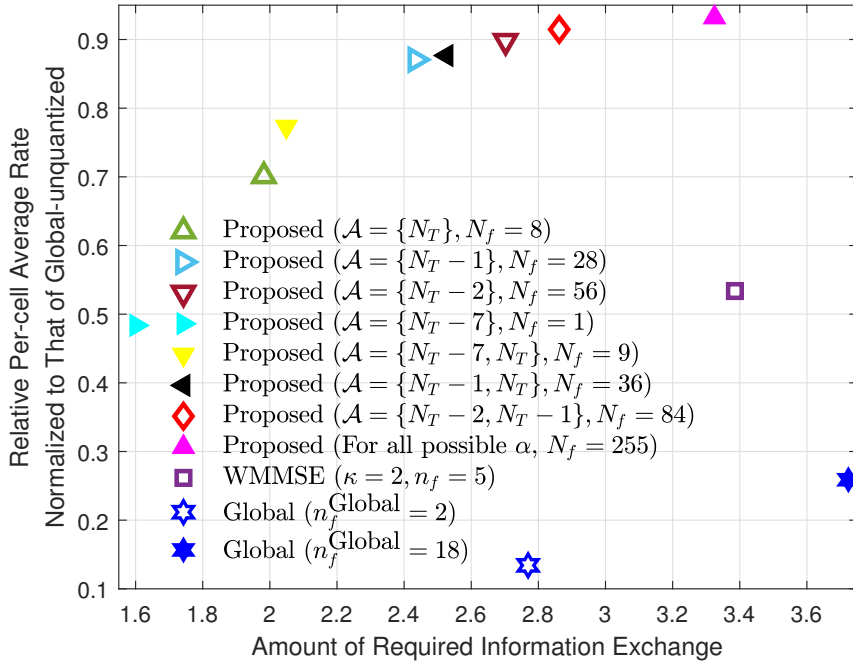


Figure 15: Probability that each α value is chosen in the proposed scheme for SNR of -5~25dB, $N_T = 8$, and $N_C = 9, 10, 11, 12$

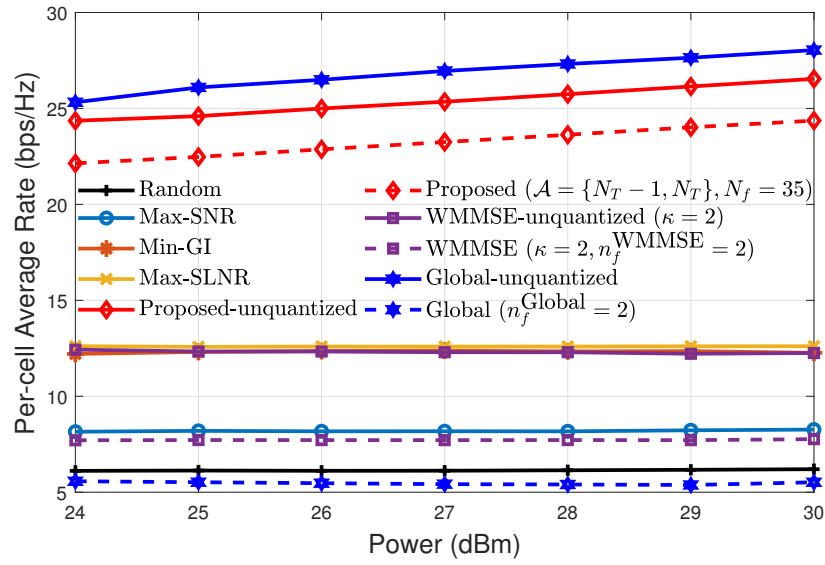


(a) $N_T = 4$ and $N_C = 7$

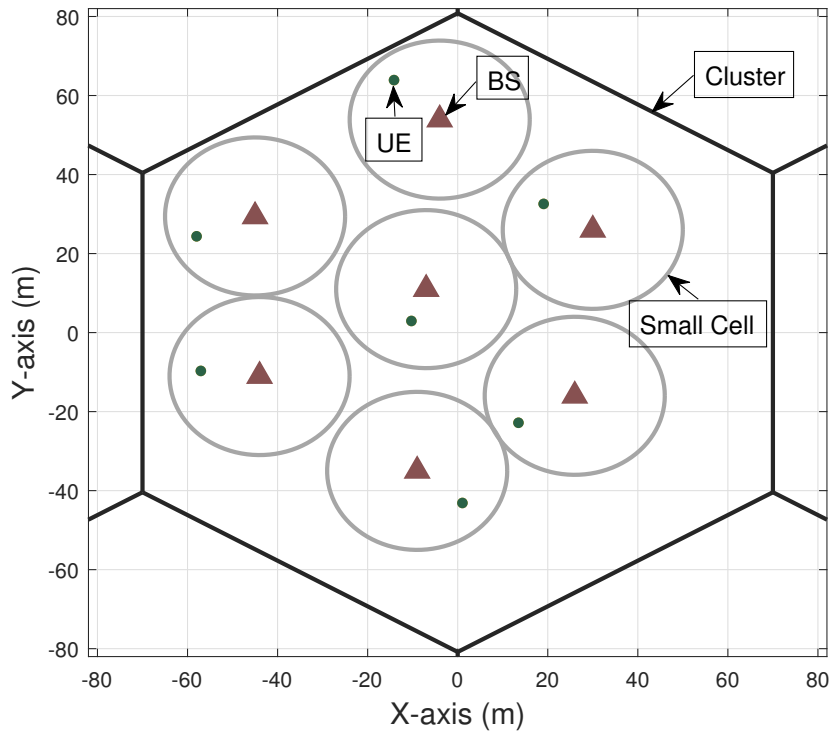


(b) $N_T = 8$ and $N_C = 9$

Figure 16: Relative per-cell average rate normalized to that of ‘Global-unquantized’ versus the amount of required information exchange for SNR of -5~25dB

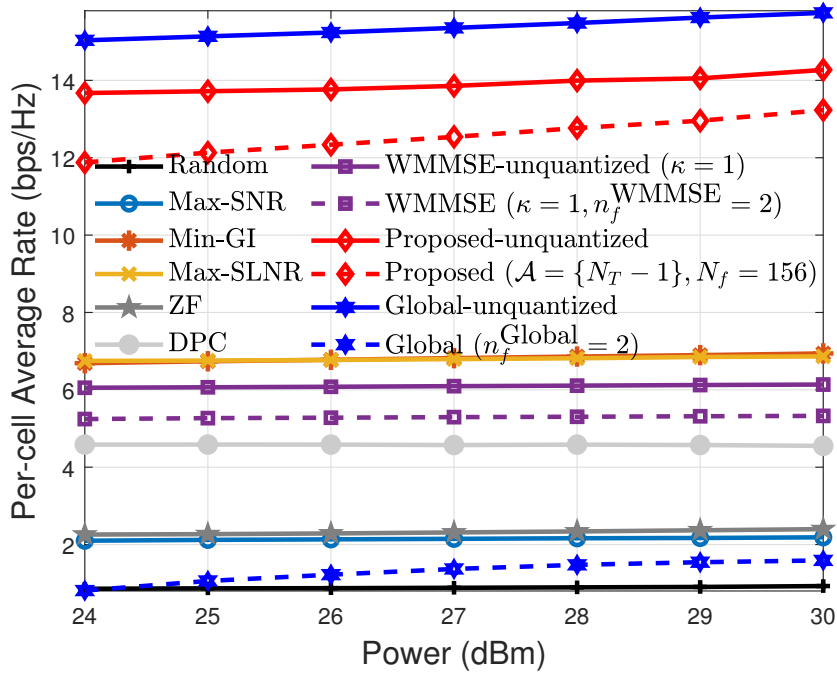


(a)

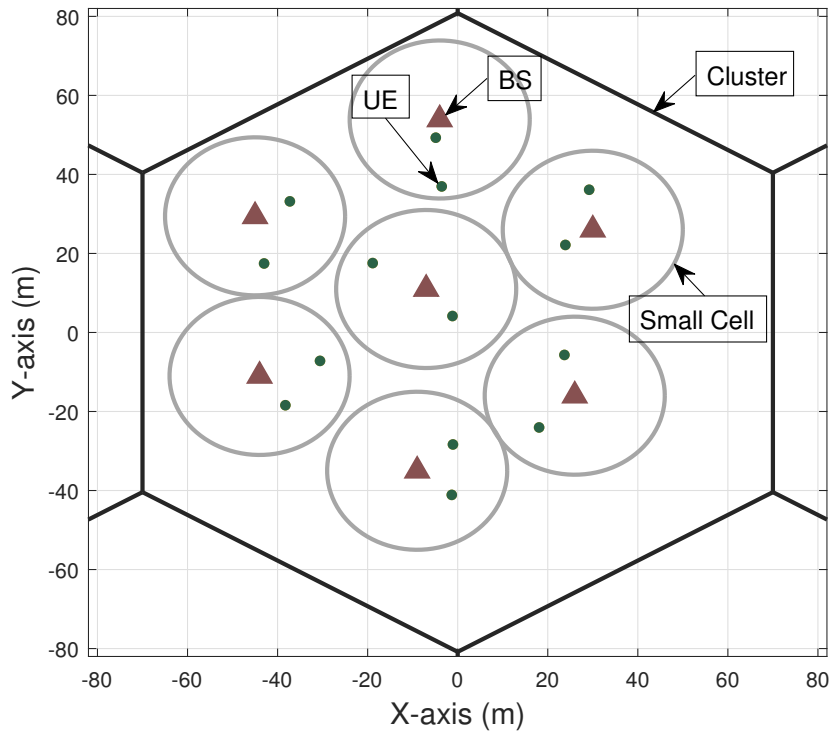


(b)

Figure 17: (a) The per-cell average rate versus transmission power and (b) the cell configuration with a single user per cell for $N_T = 4$ and $N_C = 7$



(a)



(b)

Figure 18: (a) The per-cell average rate versus transmission power and (b) the cell configuration for $N_T = 4$, $N_C = 7$, and $N_U = 2$

V Proposed Beamforming Design 3 - Selection of IFUs with DNN

In this section, the DNN architecture is used to choose the proper set of IFUs to maximize the sum-rate by solving classification problem based on supervised learning. Then, all the BSs design the beamforming vectors making interference to the selected IFUs zero which is introduced in Section IV.

5.1 Input data

The input of the overall DNN is the vector where the components are the rates $r_m^{[c]}$ in $R_{\text{local}}^{[c]}$ of (71), $c \in \mathcal{N}_K$, $m \in \mathcal{F}_c$. Note that $r_m^{[c]}$, $c \in \mathcal{N}_K$, $m \in \mathcal{F}_c$, requires only local CSI to be computed by BS m . Then, the input vector is denoted by \mathbf{x} and the size of the input vector is $N_I = \sum_{k=1}^{N_T} \binom{N_C-1}{k-1}$.

5.2 Offline training data

The DNN is trained to choose the c^* -th IFU selection which maximizes the sum-rate as follow:

$$c^* = \arg \max_{c \in \mathcal{N}_K} R^{[c]}. \quad (103)$$

Then, the training data \mathbf{y} is composed of

$$y_c = \begin{cases} 1 & \text{if } c = c^* \\ 0 & \text{if } c \in \mathcal{N}_K \setminus \{c^*\}, \end{cases} \quad (104)$$

where y_c is the c -th element of \mathbf{y} . Since global CSI is required to compute $R^{[c]}$ and get the solution of (103), the information related to (103) is used only for offline training stage.

5.3 Selection of \mathcal{F} using DNN

The DNN architecture is designed based on supervised learning for classification problem. The hidden layer in the DNN is composed of 13 fully-connected layers with 12 Relu activation functions and a softmax layer as shown in Fig. 19. The output vector size of the output layer is N_K . Let us denote the output vector which is the estimated result of DNN as $\hat{\mathbf{y}}$ and the c -th element of $\hat{\mathbf{y}}$ as \hat{y}_c . Then the loss function is defined as

$$l(\hat{\mathbf{y}}) = \|\hat{\mathbf{y}} - \mathbf{y}\| \quad (105)$$

and the DNN is trained to estimate $\hat{\mathbf{y}}$ minimizing the loss $l(\hat{\mathbf{y}})$. Finally, the \hat{c} -th IFU selection, $\mathcal{F}_{\hat{c}}$, is chosen as the final IFU selection where \hat{c} -th element has the maximum value among the N_K elements in the output vector as follow:

$$\mathcal{F} = \mathcal{F}_{\hat{c}} \quad (106)$$

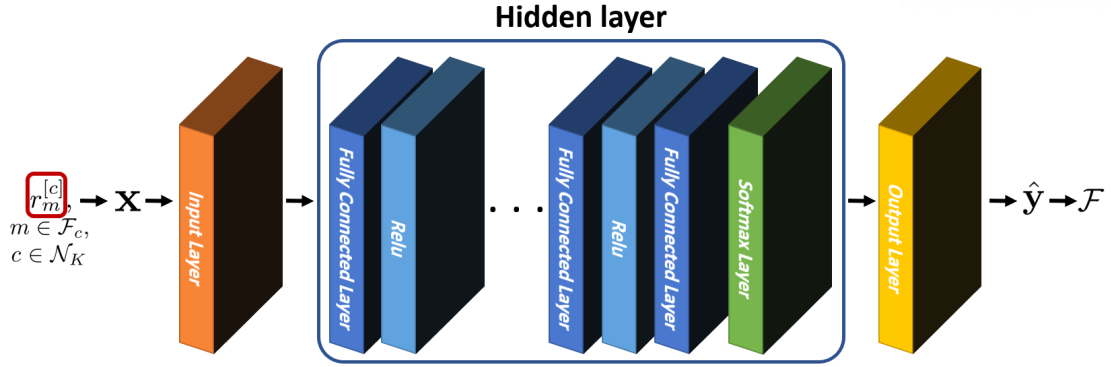


Figure 19: Proposed DNN architecture

where

$$\hat{c} = \arg \max_{c \in \mathcal{N}_K} \hat{y}_c. \quad (107)$$

5.4 Numerical Simulations

For the numerical simulation, 80000 data sets are used for the offline training and 20000 data sets are used for the test of the DNN. The proposed DNN is implemented by Python 3.7 with Tensorflow 1.14.0 and a popular library Numpy.

Figures 20a and 20b demonstrate the accuracy of the test set versus epoch in the single user small cell network [57, 59, 60] for $(N_T = 3, N_C = 4)$ and $(N_T = 4, N_C = 5)$, respectively. As shown in Figs. 20a and 20b, the accuracy of the proposed scheme increases as the number of epoch increases and converges into around 0.8 and 0.7, respectively, showing that the DNN chooses the IFU selection which is chosen with global CSI at quite high rate with only local CSI. The accuracy for $(N_T = 4, N_C = 5)$ is lower than that for $(N_T = 3, N_C = 4)$, since the number of the possible IFU selection cases for $(N_T = 4, N_C = 5)$ is larger than that for $(N_T = 3, N_C = 4)$.

In Figs. 21a and 21b, the per-cell average rate of the proposed scheme versus transmit power of BS is compared with ‘WSLNR’ and ‘Global’ for $(N_T = 3, N_C = 4)$ and $(N_T = 4, N_C = 5)$, respectively, in the single-user small cell network [57, 59, 60]. Three schemes requiring only local CSI without information exchange are also considered as follows. First, ‘Max-SNR’ is considered, in which all the beamforming vectors are designed only to maximize the channel gain of the desired channels. Second, ‘Min-GI’ [7] is considered, where all the beamforming vectors are determined only to minimize GI. Third, in ‘Max-SLNR’ [4], all the beamforming vectors are constructed maximizing SLNR. In the baseline ‘Random’ scheme, each beamforming vector is randomly determined. Besides, ‘WSLNR-global’ is considered where the IFU selection is chosen as (103), which is the result of the trained output data. To show the impact of the IFU selection of the proposed scheme, ‘WSLNR-random’ is considered where the set of IFUs is selected randomly.

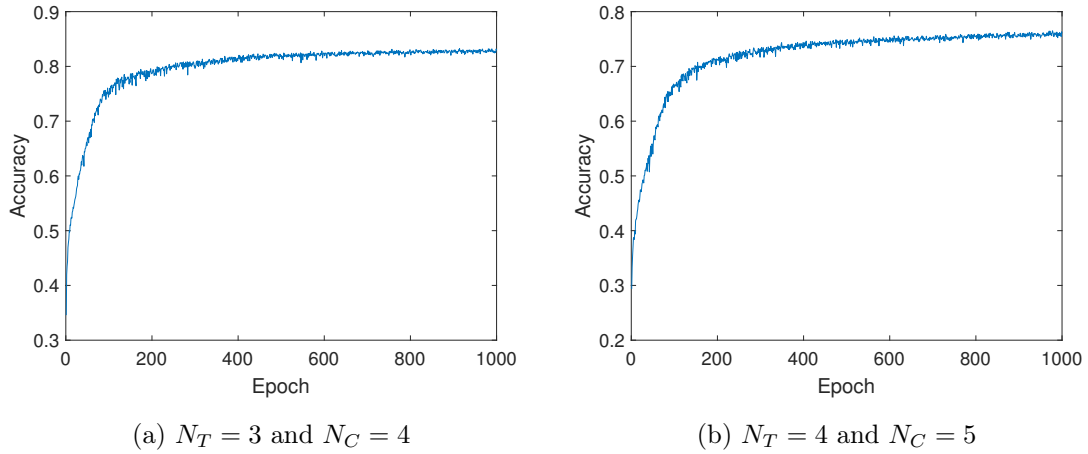
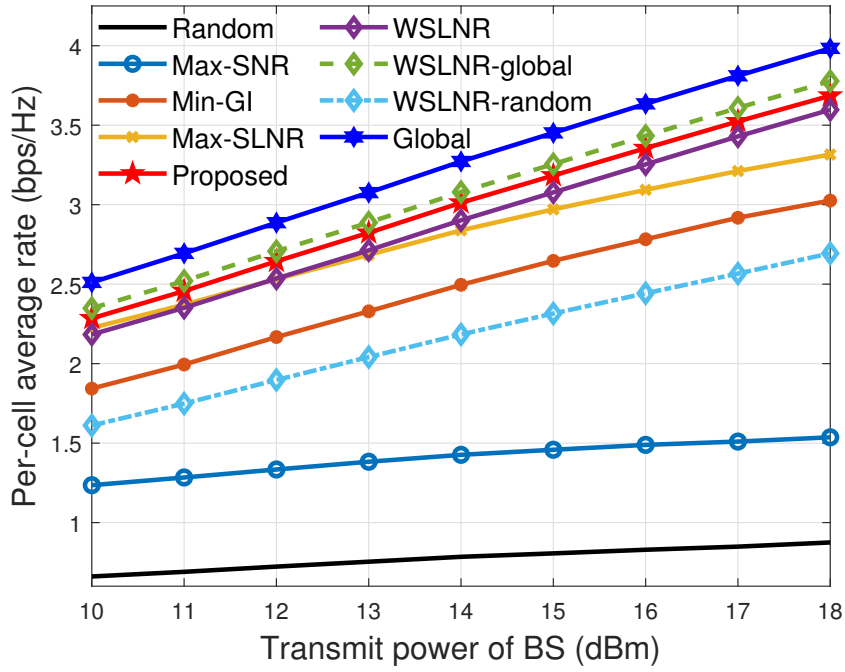
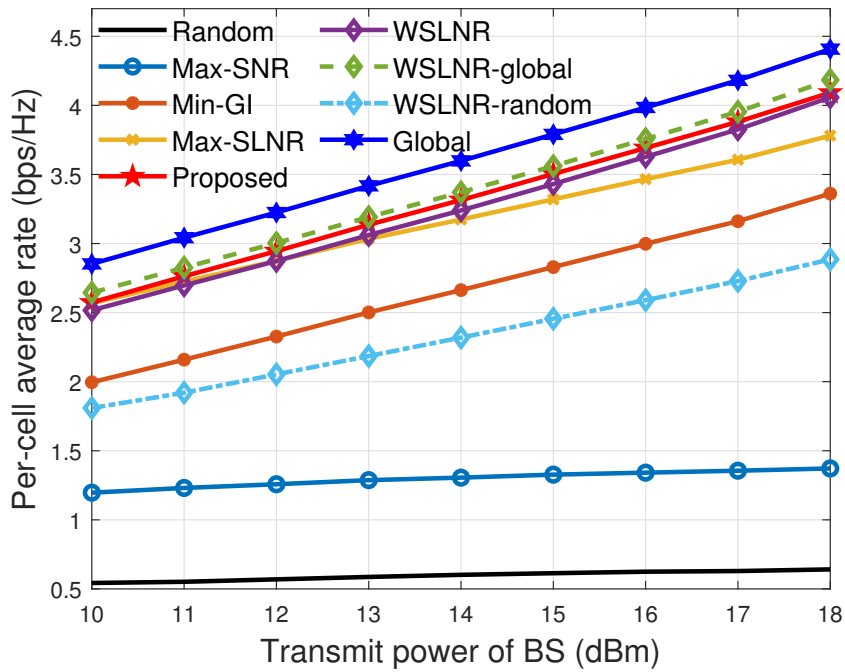


Figure 20: Accuracy of the proposed scheme for the test set versus epoch

As shown in Figs. 21a and 21b, the proposed scheme shows the highest per-cell average rate among those of the schemes which require only local CSI for all the considered transmit power of BS. The proposed scheme achieves a close per-cell average rate to that of ‘WSLNR-global’ which is the result of trained data showing that the DNN is well trained to capture the partial CSI which cannot be figured out with local CSI. The gap of the per-cell average rates of the proposed scheme and ‘WSLNR’ shows the improvement of the DNN compared to ‘WSLNR’ with the same amount of information exchange and local CSI.



(a) $N_T = 3$ and $N_C = 4$



(b) $N_T = 4$ and $N_C = 5$

Figure 21: Per-cell average rate versus transmit power of BSs

VI Conclusion

We have proposed a non-iterative beamforming design scheme based on limited information exchange among the BSs to improve the sum-rate of the MISO interference channel. The proposed beamforming designs only require local CSI and limited scalar information exchange between the BSs. Though there have been several schemes in which the beamforming vector is designed with limited backhaul signaling between the BSs, for given amount of backhaul signaling, the proposed schemes significantly outperforms the existing schemes in the overall SNR regime. Unlike a few previous schemes, the proposed schemes require no iterative design between the transmitters and receivers, and the amount of information exchange does not increase as the number of antennas grows. These aforementioned benefits make the proposed schemes suitable in practical MISO interference channels. The key aspects of the proposed schemes are summarized as follows:

6.1 First work

The concept of WGI has been introduced. Through local CSI and a few scalar information exchanges between BSs, the sum-rate can be increased by properly designing the weight coefficients of WGI. By minimizing the WGI with the proper weight coefficients, the proposed scheme achieves higher per-cell average rate with lower amount of information exchange as shown in the simulation result.

6.2 Second work

- **IFUs:** Turning off a set of BSs has been introduced as one of the technologies to improve sum-rate in 3GPP. We have definitized this technology by introducing a notion of IFUs who shall receive zero intercell interference via multicell transmit beamforming requiring very low information exchange. By selecting the proper number of the IFUs and the proper set of IFUs, near-optimal sum-rates are achieved as shown in the simulation results.
- **Exchange of limited scalar information:** In the proposed scheme, the information exchange protocol requires only scalar information exchange among the BSs with the proposed quantization method. The beamforming vectors are designed in each coherence time of 10 ms to 100 ms, then the required information exchange of the proposed scheme is 1-200kbps which is much smaller than the limited direct link capacity defined by 3GPP, 10 Mbps to 100Mbps. With the highly limited exchanged information, the proposed scheme closely achieves the optimal sum-rate bound, significantly outperforming the existing schemes in almost all the SNR regime. Unlike previous schemes, the proposed scheme requires no iterative beamforming design between the transmitters and receivers and no vector information exchange. These aforementioned benefits make the proposed scheme suitable in practical MISO interference networks.

- **Multiuser case:** The extension of the proposed scheme to the multiuser case also has been derived. Simulation results show that the proposed scheme outperforms the existing schemes with highly limited information exchange in multiuser networks.
- **Future work:** Our future study will focus on extending the idea to the multiuser MIMO interference channel. In the proposed scheme, some of the users inevitably may have relatively low achievable rates to maximize the total sum-rate. In the future work, the sum-rate maximizing beamforming optimization problem will be considered with the constraints on the minimum quality of service of users.

6.3 Third work

The DNN is applied to the beamforming vector design to maximize the sum-rate. By choosing the proper set of IFUs with DNN based on supervised learning, the sum-rate can be maximized. The input of the DNN is designed as the set of scalar information exchanged between the BSs that can be calculated with only local CSI by each BS. The proposed DNN has been solved the classification problem. By designing the problem as the classification problem which chooses the proper set of IFUs, the network is trained faster and better.

References

- [1] Y. Kim, H. J. Yang, and H. Jwa, "Multicell downlink beamforming with limited backhaul signaling," *IEEE Access*, vol. 6, pp. 64 122–64 130, Oct. 2018.
- [2] Y. Kim and H. J. Yang, "Sum-rate maximization of multicell miso networks with limited information exchange," *IEEE Transactions on Vehicular Technology*, Mar. 2020.
- [3] A. K. Gupta, X. Zhang, and J. G. Andrews, "SINR and throughput scaling in ultradense urban cellular networks," *IEEE wireless commun. lett.*, vol. 4, no. 6, pp. 605–608, Dec. 2015.
- [4] E. Björnson, R. Zakhour, D. Gesbert, and B. Ottersten, "Cooperative multicell precoding: Rate region characterization and distributed strategies with instantaneous and statistical CSI," *IEEE Trans. Signal Process.*, vol. 58, no. 8, pp. 4298–4310, Aug. 2010.
- [5] R. Bhagavatula, R. W. Heath, Jr., and B. Rao, "Limited feedback with joint CSI quantization for multicell cooperative generalized eigenvector beamforming," in *Proc. IEEE ICASSP*, Dallas, TX, Mar. 2010, pp. 2838–2841.
- [6] T. Kim, D. J. Love, and B. Clerckx, "On the spatial degrees of freedom of multicell and multiuser MIMO channels," *arXiv*, 2016. [Online]. Available: <http://arxiv.org/abs/1111.3160v2>
- [7] H. J. Yang, W.-Y. Shin, B. C. Jung, C. Suh, and A. Paulraj, "Opportunistic downlink interference alignment for multi-cell MIMO networks," *IEEE Trans. Wireless Commun.*, vol. 16, no. 3, pp. 1533–1548, Mar. 2017.
- [8] C. Suh, M. Ho, and D. N. C. Tse, "Downlink interference alignment," *IEEE Trans. Commun.*, vol. 59, no. 9, pp. 2616–2626, Sep. 2011.
- [9] E. A. Jorswieck, E. G. Larsson, and D. Danev, "Complete characterization of the pareto boundary for the MISO interference channel," *IEEE Trans. Signal Process.*, vol. 56, no. 10, pp. 5292–5296, Oct. 2008.
- [10] T. Gou and S. A. Jafar, "Degrees of freedom of the K user M x N MIMO interference channel," *IEEE Trans. Inf. Theory*, vol. 56, no. 12, pp. 6040–6057, Dec. 2010.
- [11] "Requirements for further advancements for E-UTRA (LTE-Advanced)," 3GPP TR 36.913, Release 13, Jun. 2018.

- [12] “Coordinated multi-point operation for LTE physical layer aspects,” 3GPP TR 36.819, Release 11, Sep. 2013.
- [13] V. R. Cadambe and S. A. Jafar, “Interference alignment and degrees of freedom of the K-user interference channel,” *IEEE Trans. Inf. Theory*, vol. 54, no. 8, pp. 3425–3441, Aug 2008.
- [14] A. Goldsmith, S. A. Jafar, N. Jindal, and S. Vishwanath, “Capacity limits of MIMO channels,” *IEEE J. Select. Areas in Commun.*, vol. 21, no. 5, pp. 684–702, June 2003.
- [15] L. Lu, G. Y. Li, A. L. Swindlehurst, A. Ashikhmin, and R. Zhang, “An overview of massive MIMO: Benefits and challenges,” *IEEE J. Sel. Topics Signal Process.*, vol. 8, no. 5, pp. 742–758, Oct 2014.
- [16] H. Tabassum, A. H. Sakr, and E. Hossain, “Analysis of massive MIMO-enabled downlink wireless backhauling for full-duplex small cells,” *IEEE Trans. Commun.*, vol. 64, no. 6, pp. 2354–2369, June 2016.
- [17] “Study on new radio access technology physical layer aspects,” 3GPP TR 38.802, Release 14, Sep. 2017.
- [18] “Small cell enhancements for E-UTRA and E-UTRAN - physical layer aspects,” 3GPP TR 36.872, Release 12, Dec. 2013.
- [19] S. A. Jafar and M. J. Fakhreddin, “Degrees of freedom for the MIMO interference channel,” *IEEE Trans. Inf. Theory*, vol. 53, no. 7, pp. 2637–2642, July 2007.
- [20] S. He, Y. Huang, and L. Yang, “Coordinated beamforming for sum rate maximization in multi-cell downlink systems,” *Signal Processing*, vol. 105, pp. 22–29, Dec. 2014.
- [21] E. G. Larsson and E. A. Jorswieck, “Competition versus cooperation on the MISO interference channel,” *IEEE J. Select. Areas in Commun.*, vol. 26, no. 7, pp. 1059–1069, Sep. 2008.
- [22] F. Shi, W. Xu, and C. Zhao, “A limited feedback strategy for cooperative multicell MISO systems,” in *Proc. WCSP*, Nanjing, China, Nov. 2011.
- [23] H. Song, Q. Yang, K. S. Kwak, F. Fu, and P. Zhu, “Joint beamforming for multi-cell MISO interference channel with limited feedback,” in *Proc. ISCIT*, Tokyo, Japan, Oct. 2010, pp. 907–910.
- [24] J. Mirza, P. J. Smith, and P. A. Dmochowski, “Coordinated regularized zero-forcing precoding for multicell MISO systems with limited feedback,” *IEEE Trans. Vehi. Technol.*, vol. 66, no. 1, pp. 335–343, Jan. 2017.

- [25] O. Simeone, O. Somekh, H. V. Poor, and S. Shamai (Shitz), “Downlink multicell processing with limited-backhaul capacity,” *EURASIP J. Adv. Signal Process.*, pp. 1–10, 2009.
- [26] R. Bhagavatula and R. W. Heath, Jr., “Adaptive limited feedback for sum-rate maximizing beamforming in cooperative multicell systems,” *IEEE Trans. Signal Process.*, vol. 59, no. 2, pp. 800–811, Feb. 2011.
- [27] Y. Wu, T. Wang, Y. Sun, and Y. Cui, “Limited feedback for cooperative multicell MIMO systems with multiple receive antennas,” *IEICE Trans. on Commun.*, vol. E97.B, no. 8, pp. 1701–1708, Aug. 2014.
- [28] S. Mosleh, J. D. Ashdown, J. D. Matyjias, M. J. Medley, J. Zhang, and L. Liu, “Interference alignment for downlink multi-cell LTE-advanced systems with limited feedback,” *IEEE Trans. Wireless Commun.*, vol. 15, no. 12, pp. 8107–8121, Dec. 2016.
- [29] S. Balaji and P. Mallick, “Performance analysis of adaptive limited feedback coordinated zero-forcing multicell systems in time-varying channels: A practical approach,” *Int’l J. of Commun. Sys.*, vol. 30, no. 14, p. e3301, Mar. 2017.
- [30] N. Lee and W. Shin, “Adaptive feedback scheme on K-cell MISO interfering broadcast channel with limited feedback,” *IEEE Trans. Wireless Commun.*, vol. 10, no. 2, pp. 401–406, Feb. 2011.
- [31] S. Balaji and P. S. Mallick, “On the optimality of multi-user coordinated zero-forcing beamforming multicell systems with limited feedback in interference channels,” *Wireless Personal Commu.*, vol. 98, no. 1, pp. 521–540, Jan. 2018.
- [32] J. Kaleva, A. Tölli, M. J. Juntti, R. Berry, and M. L. Honig, “Joint transmission with limited backhaul connectivity,” *arXiv*, 2017. [Online]. Available: <http://arxiv.org/abs/1705.05252>
- [33] X. Chen and C. Yuen, “On interference alignment with imperfect CSI: Characterizations of outage probability, ergodic rate and SER,” *IEEE Trans. Vehi. Technol.*, vol. 65, no. 1, pp. 47–58, Jan. 2016.
- [34] N. Hassanpour, J. E. Smee, J. Hou, and J. B. Soriaga, “Distributed beamforming based on signal-to-caused-interference ratio,” in *Proc. IEEE Int’l Symp. Spread Spectrum Tech. and Appl.*, Bologna, Italy, Aug. 2008, pp. 405–410.
- [35] R. Zakhour and D. Gesbert, “Distributed multicell-MISO precoding using the layered virtual SINR framework,” *IEEE Trans. Wireless Commun.*, vol. 9, no. 8, pp. 2444–2448, Aug. 2010.
- [36] B. O. Lee, H. W. Je, I. Sohn, O.-S. Shin, and K. B. Lee, “Interference-aware decentralized precoding for multicell MIMO TDD systems,” in *Proc. IEEE Globecom*, New Orleans, LA, Nov.-Dec. 2008, pp. 1–5.

- [37] M. Sadek, A. Tarighat, and A. H. Sayed, “A leakage-based precoding scheme for downlink multi-user MIMO channels,” *IEEE Trans. Wireless Commun.*, vol. 6, no. 5, pp. 1711–1721, May 2007.
- [38] R. Zakhour and D. Gesbert, “Coordination on the MISO interference channel using the virtual SINR framework,” in *Proc. International ITG Workshop on Smart Antennas*, Berlin, Germany, Feb. 2009.
- [39] L. Qiang, Y. Yang, F. Shu, and W. Gang, “Coordinated beamforming in downlink CoMP transmission system,” in *Proc. Int’l ICST Conf. on Commun. and Networking in China*, Aug. 2010.
- [40] C. Shi, D. A. Schmidt, R. A. Berry, M. L. Honig, and W. Utschick, “Distributed interference pricing for the MIMO interference channel,” in *Proc. IEEE ICC*, Dresden, Germany, Jun. 2009.
- [41] A. Tölli, H. Pennanen, and P. Komulainen, “Decentralized minimum power multi-cell beamforming with limited backhaul signaling,” *IEEE Trans. Wireless Commun.*, vol. 10, no. 2, pp. 570–580, Feb. 2011.
- [42] Y. Xu, C. He, L. Jiang, and J. Li, “Distributed dynamic SINR pricing for multi-cell beamforming with limited backhaul signaling,” in *Proc. IEEE Globecom*, Atlanta, GA, Dec. 2013, pp. 3620–3624.
- [43] D. H. N. Nguyen and T. Le-Ngoc, “Multiuser downlink beamforming in multicell wireless systems: A game theoretical approach,” *IEEE Trans. Signal Process.*, vol. 59, no. 7, pp. 3326–3338, Jul. 2011.
- [44] Q. Shi, M. Razaviyayn, Z.-Q. Luo, and C. He, “An iteratively weighted MMSE approach to distributed sum-utility maximization for a MIMO interfering broadcast channel,” *IEEE Trans. Signal Process.*, vol. 59, no. 9, pp. 4331–4340, Sep. 2011.
- [45] W. Xia, G. Zheng, Y. Zhu, J. Zhang, J. Wang, and A. P. Petropulu, “A deep learning framework for optimization of MISO downlink beamforming,” *IEEE Trans. on Commun.*, vol. 68, no. 3, pp. 1866–1880, 2020.
- [46] H. J. Yang, W.-Y. Shin, B. C. Jung, C. Suh, and A. Paulraj, “Opportunistic downlink interference alignment,” *arXiv*, Preprint. [Online available at <http://arxiv.org/pdf/1312.7198v2.pdf>].
- [47] L. Y. Kolotilina, “The strengthened versions of the additive and multiplicative Weyl inequalities,” *Journal of Mathematical Sciences*, vol. 127, no. 3, pp. 1976–1987, 2005.
- [48] S. P. Lloyd, “Least squares quantization in PCM,” *IEEE Trans. Inf. Theory*, vol. 28, no. 2, pp. 129–137, Mar. 1982.

- [49] T. Ratnarajah, R. Vaillancourt, and M. Alvo, “Eigenvalue and condition numbers of complex random matrices,” *SIAM Journal on Matrix Analysis and Applications*, vol. 26, no. 2, pp. 441–456, Jan. 2005.
- [50] N. Jindal, “MIMO broadcast channels with finite-rate feedback,” *IEEE Trans. Inf. Theory*, vol. 52, no. 11, pp. 5045–5060, Nov. 2006.
- [51] T. Tao and V. Vu, “Random matrices: The distribution of the smallest singular values,” *Geometric and Functional Analysis*, vol. 20, pp. 260–297, Jun. 2010.
- [52] A. Hjørungnes, J. Akhtar, and D. Gesbert, “Precoding for space-time block codes in (non-)kronecker correlated MIMO channels,” in *European Signal Processing Conference*, Vienna, Austria, Sep. 2004, pp. 515–518.
- [53] C. M. Yetis, T. Gou, S. A. Jafar, and A. H. Kayran, “On feasibility of interference alignment in MIMO interference networks,” *IEEE Trans. Signal Process.*, vol. 58, no. 9, pp. 4771–4782, Sep. 2010.
- [54] S. Abramovich and L.-E. Persson, “Some new estimates of the ‘Jensen gap’,” *J. Inequal. Appl.*, vol. 2016, no. 1, Feb. 2016.
- [55] X. Gao, M. Sitharam, and A. E. Roitberg, “Bounds on the Jensen gap, and implications for mean-concentrated distributions,” *arXiv*, 2018. [Online]. Available: <http://arxiv.org/abs/1712.05267v3>
- [56] Z.-H. Sun, “Inequalities for binomial coefficients,” *arXiv*, 2013. [Online]. Available: <http://arxiv.org/abs/1111.3160v2>
- [57] “RF requirements for LTE pico node B,” 3GPP TR 36.931, Release 13, Jun. 2018.
- [58] M. H. M. Costa, “Writing on dirty paper (corresp.),” *IEEE Trans. Inf. Theory*, vol. 29, no. 3, pp. 439–441, May 1983.
- [59] “Spatial channel model for multiple input multiple output (mimo) simulations,” 3GPP TR 25.996, Release 15, Jun. 2018.
- [60] “Further advancements for E-UTRA physical layer aspects,” 3GPP TR 36.814, Release 9, Mar. 2017.

